

QA of absorbed dose and RBE in contemporary radiotherapy

Professor Anatoly B. Rozenfeld

CENTRE FOR
MEDICAL
RADIATION PHYSICS 

UNIVERSITY OF
WOLLONGONG



Acknowledgement

Special acknowledgement to our partners :

- ▶ **SPA BIT** CMRP exclusive semiconductor foundry
- ▶ **ICCC:** Illawarra Cancer Care Centre, Wollongong

This work will be impossible without large number of PhD students at CMRP who are essentially contributing to all results.

CMRP PhD students: I. Fuduli, M. Weaver, A. Espinoza...

Uni Wisconsin Prof Wolfgang Tome (USA) ,

Peter MacCalum CC AU Prof Tomas Kron, Dr Nick Hardcastle,

LLUMC proton therapy centers, USA (Prof R Schulte, Dr A.Wroe)

University Malaya , Dr J Wong, Prof Ng

Prague TU , Prof Pospisil, Dr J Jacubeck

ANSTO: Drs D. Prokopovich , M. Reinhard

CMRP: Drs M.Petasecca, M.Carolan, S.Guatelli , Prof P Metcalfe, A/Prof M.Lerch

Hospitals partnership: ICCC, St George CCC, POWH and Liverpool Hospital ,
Australia, MSKCC, MGH, LLUMC (USA), Heidelberg (Germany), NIRS (Japan)

NCC Milan, (Italy),



Introduction

- ▶ Advanced radiotherapy techniques such as IMRT, SRS, Helical TomoTherapy and VMAT produce radiation dose maps with high dose modulation and tight gradients.
- ▶ Difficulties in the dosimetric verification of these new complex treatment methods using existing dosimeters has led to the need for a new generation of fast responding real time dosimeters with submillimetre precision.
- ▶ Silicon Radiation Detection Systems (SRDS), designed, fabricated and prototyped by the CMRP were developed to address these needs
- ▶ **Most of them is spin off from HEP radiation detectors for fundamental research.**

Centre for Medical Radiation Physics

University of Wollongong

5 Faculties, 22,000 students, Technology Park, IHMRI, Wollongong Hospital (ICCC) and 3 more hospitals associated

Where are we?



Meet the CMRP team



Prof Anatoly Rozenfeld
Founder and Director



A/Prof Michael
Lerch



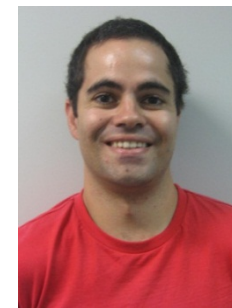
Dr George
Takacs



Dr Iwan
Cornelius



Prof Peter
Metcalfe



Dr Dean
Cutajar



Dr Marco
Petasecca



Sonny Spargo
Admin Officer
and PA



Dr Susanna
Guatelli



Dr Mitra
Safavi-Naieni



Dr Yujin Qi



Dr Elise Pogson



Michael Weaver



Dr Engbang Li



Dr Alessandra
Malaroda

Dr Linh
Tran



Dr Moeava
Tehei

Outline

- ▶ Semiconductor Dosimetry in RT
 - Diodes Design and its Applications in IMRT, SRS, Tomo
 - Dose Magnifying Glass
 - Magic Plate
 - MOSFET, *MOSkin* Design and its Applications
 - Skin Dosimetry in Radiotherapy
 - Brachytherapy Applications
 - IMRT and 3D CRT Applications
- ▶ 2D Si High Spatial Resolution Dosimetry
 - Movable targets QA dosimetry
 - Medipix-Eye plaque QA
- ▶ Electronic Dosimetry in MRT and Hadron Therapy
 - Si microdosimetry (example)
 - Micron resolution detectors
- ▶ Conclusion



Accidents in Radiotherapy



SFR Business Team, marque du groupe SFR, est à destination des entreprises. Détails et ce

Mise à jour 03:25

LE FIGARO · fr

ACTUALITÉ ÉCONOMIE CULTU

INFO

- > Politique
- > International
- > Environnement
- > Sciences
- > Auto
- > Société
- > Médias
- > Tech et Web
- > Santé
- > Météo

DÉBATS

- > Figaro I
- > Vos réa

Exemples : Médias, Présidentielle, Auto, Golf, Immobilier

EN CE MOMENT : Crise de la dette > JMJ > Affaires DSK > Primaire PS > Guerre en Libye

Radiothérapie à Epinal : un cinquième patient est mort

Un homme de 84 ans, qui faisait partie des 24 patients surirradiés à l'hôpital d'Epinal, est mort il y a une quinzaine de jours. L'information, révélée par Le Parisien, a été confirmée par Patrick Colombel, le directeur par intérim de l'établissement, qui reste prudent sur les causes du décès : "on ne sait pas s'il est lié à l'accident de radiothérapie ou non", car il était âgé et atteint d'un cancer.

Date: November 2004

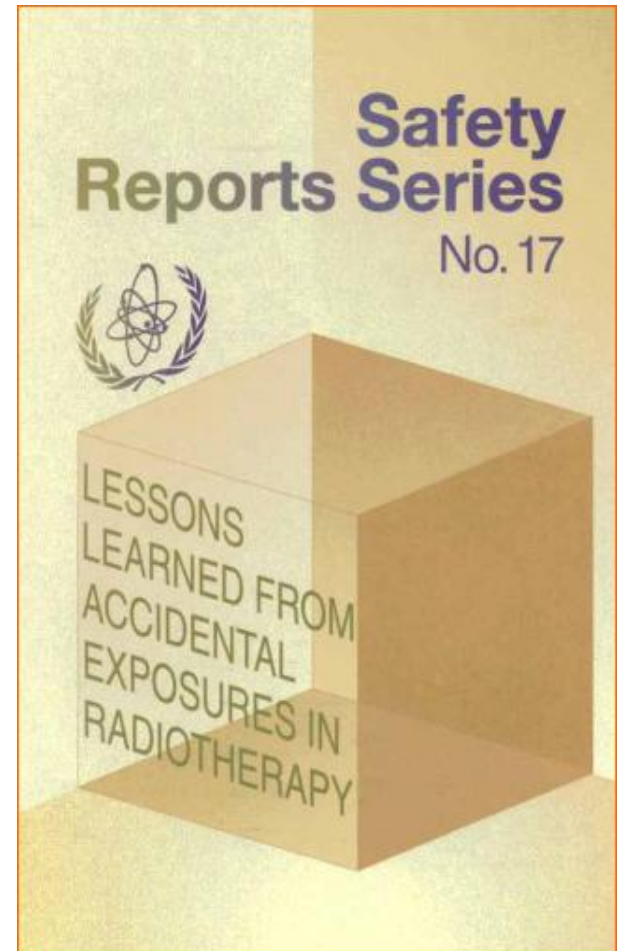
Location: Lyon, France

Type of event: radiotherapy overexposure

Description: A patient receiving treatment by radiotherapy was overexposed due to confusion over units used in defining the body surface to be irradiated.

New technology required for QA in real time

- ▶ More than 90 cases documented
 - ▶ Affects brachytherapy, external beam radiotherapy and CT scanning
 - ▶ Affects developed and developing countries
- Radiation technology for cancer treatment became **very conformal and very complex** and more rely upon computer control .
- **Large gap between delivery technology and QA**



Magic Plate

CENTRE FOR
MEDICAL
RADIATION PHYSICS



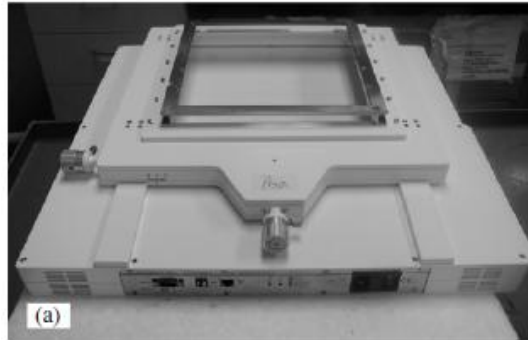
UNIVERSITY OF
WOLLONGONG



Current IMRT & VMAT verification

▶ Fluence

- DAVID system
- IBA compass



▶ In phantom

- 2D arrays – (Delta4, ArcCheck)
- MapCheck

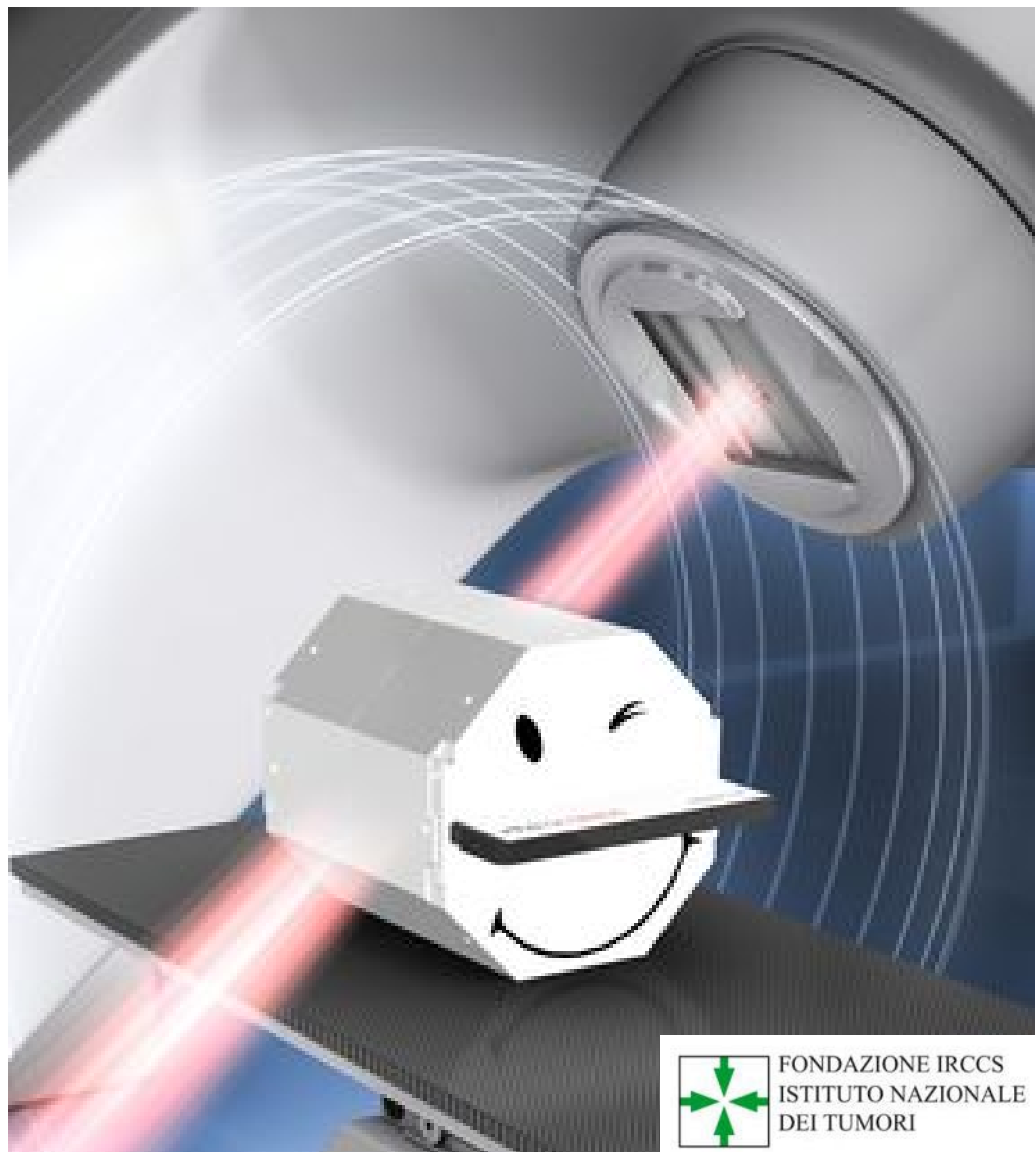


▶ Exit fluence

- EPID

SRS Arc delivery: In phantom dose measurement

- 2D detectors array plane
- Spatial resolution 5mm is poor
- New solution by CMRP

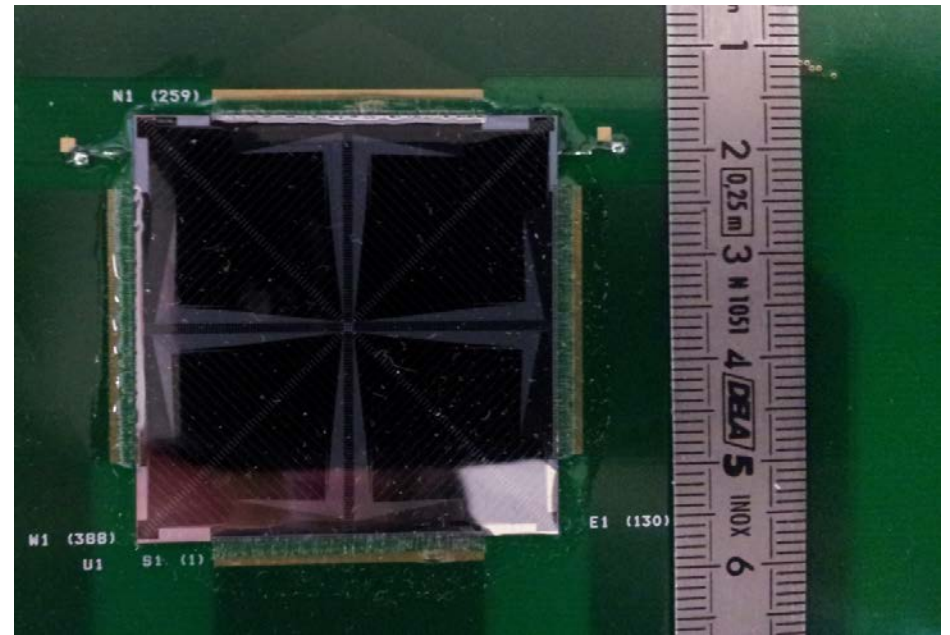
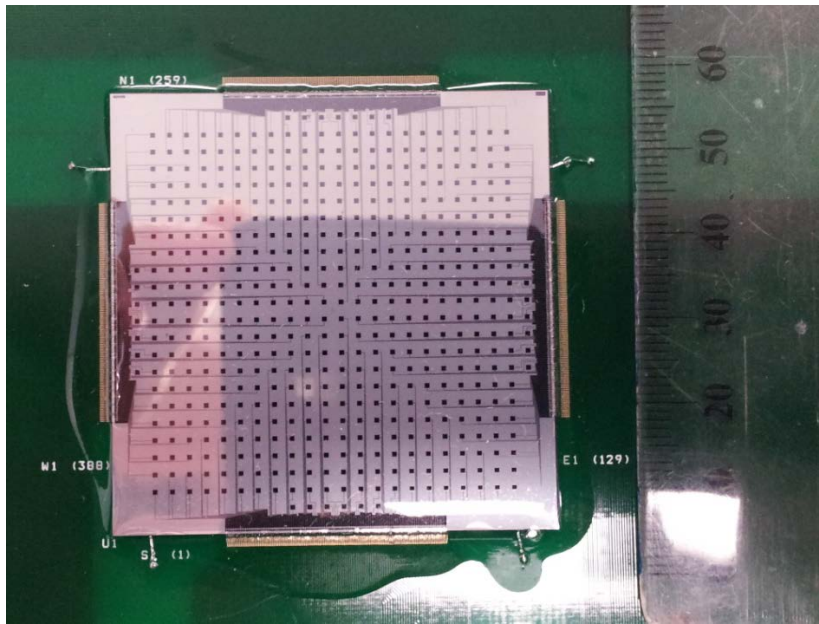


FONDAZIONE IRCCS
ISTITUTO NAZIONALE
DEI TUMORI



2D High T-S Resolution MP512 and DMG OCTA Dosimeters

- ▶ Bulk silicon substrate
- ▶ **M512 matrix:** 512 individual channels in a monolithic sensor, s-resolution 2mm, t=0.1ms
- ▶ **DMG OCTA:** 8 linear radial arrays, s-resolution 0.32 mm , t=0.1ms, shifted 45 deg.



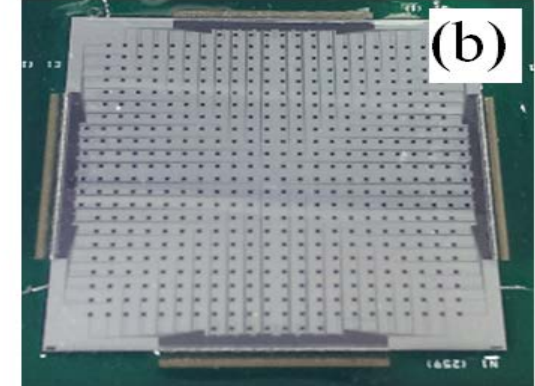
1D and 2D High T-S Resolution Dosimeters

a) **sDMG**-serial DMG: SR 0.2mm

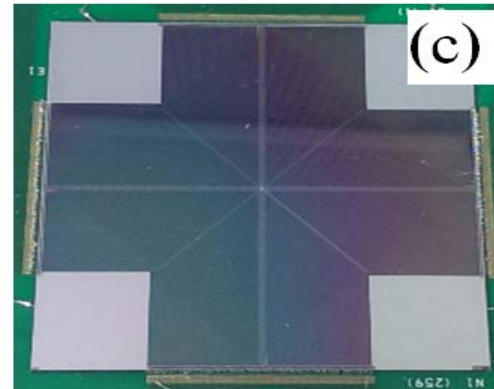


b) **MP M512** matrix: 512

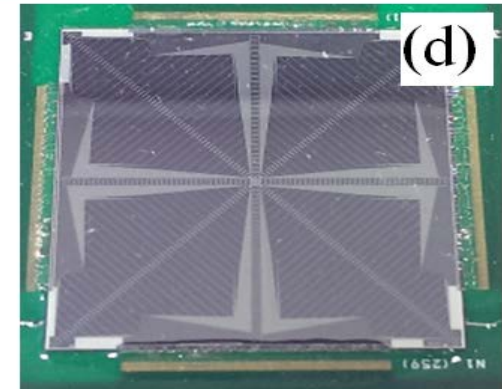
0.3x0.3mm² detectors in a
monolithic sensor, SR: 2mm



c) **DMG OCTA**: 512 0.02x0.5mm²
detectors in 8 linear radial arrays,
SR: 0.32 mm



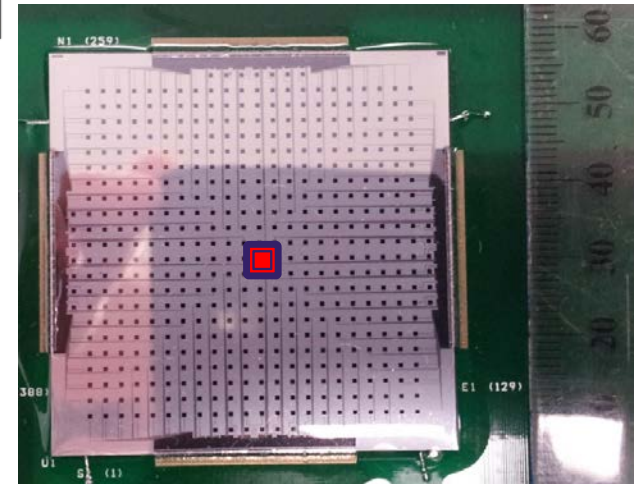
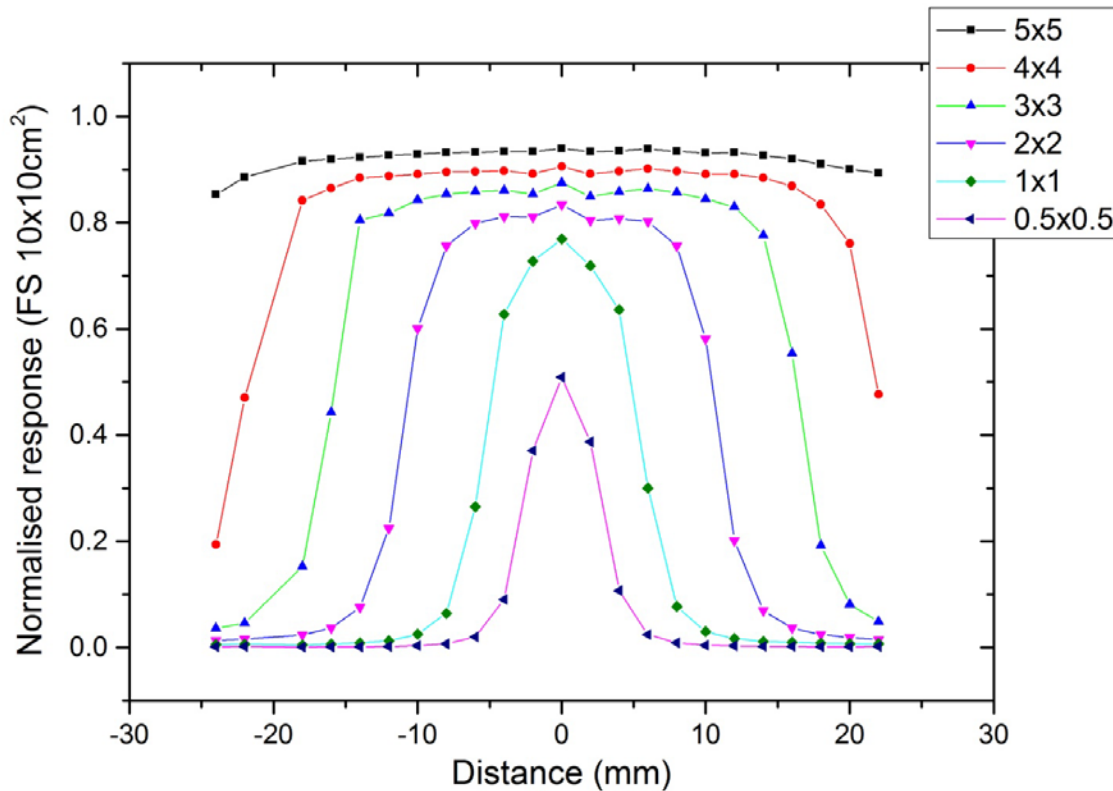
d) **DMG DUO**: 512 0.02x0.5mm²
detectors in 8 linear radial arrays,
SR: 0.2 mm



Applications:

- In phantom QA: small static and movable targets
- In Vivo real time QA: Transition mode upstream of the patient

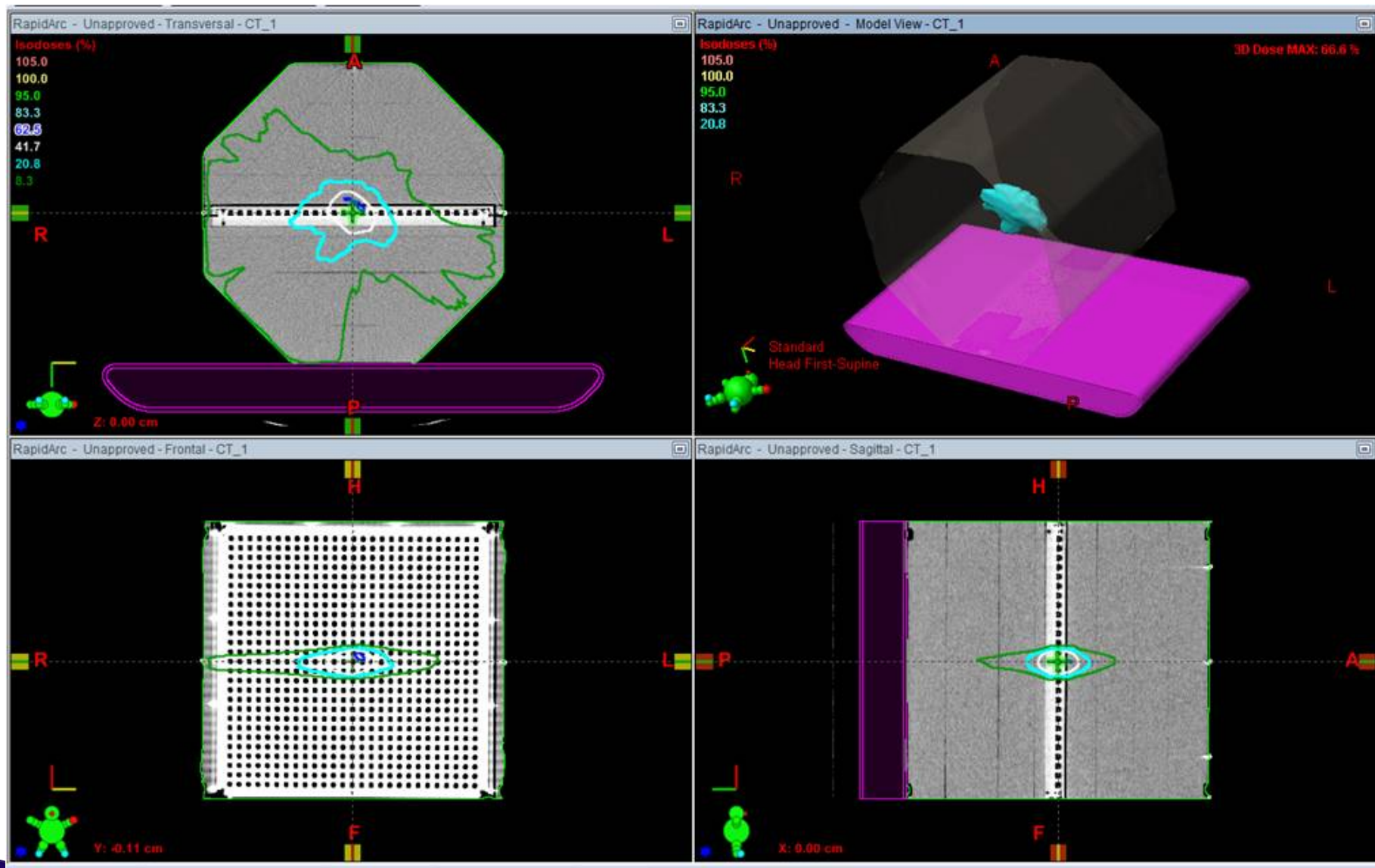
SRS Small field dosimetry with M512



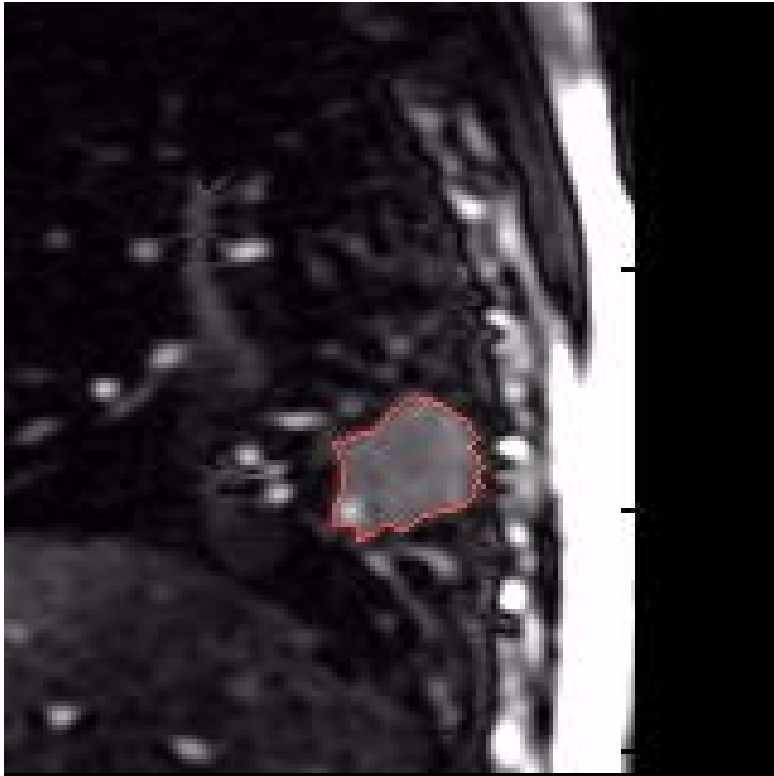
- Beam energy: 6 MV
- Depth: 10 cm
- SSD: 90 cm (isocentre)



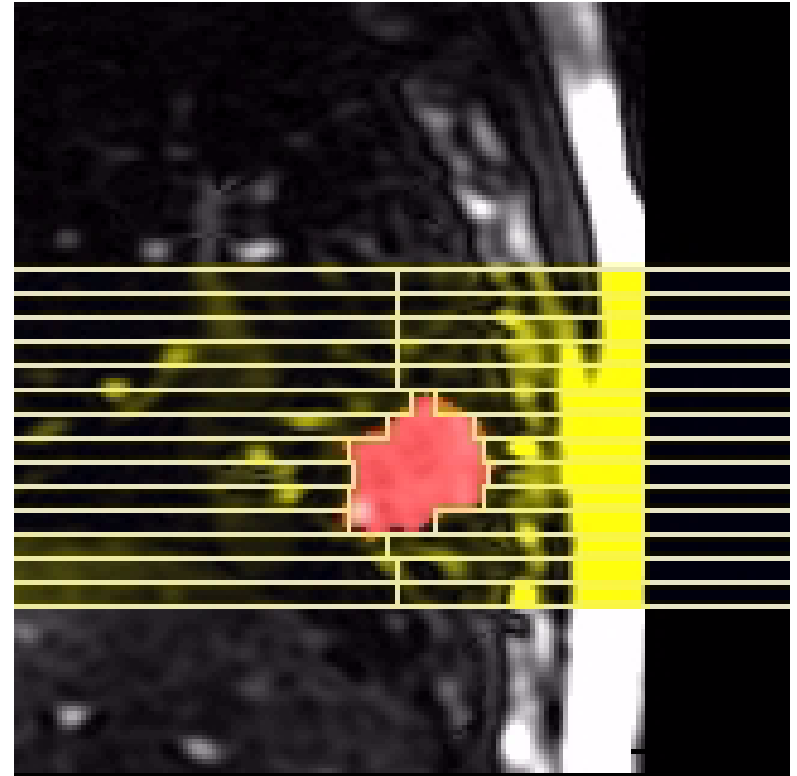
SRS :In phantom dose calculation with CMRP MP M512



QA Dosimetry for Motion Adaptive Therapy

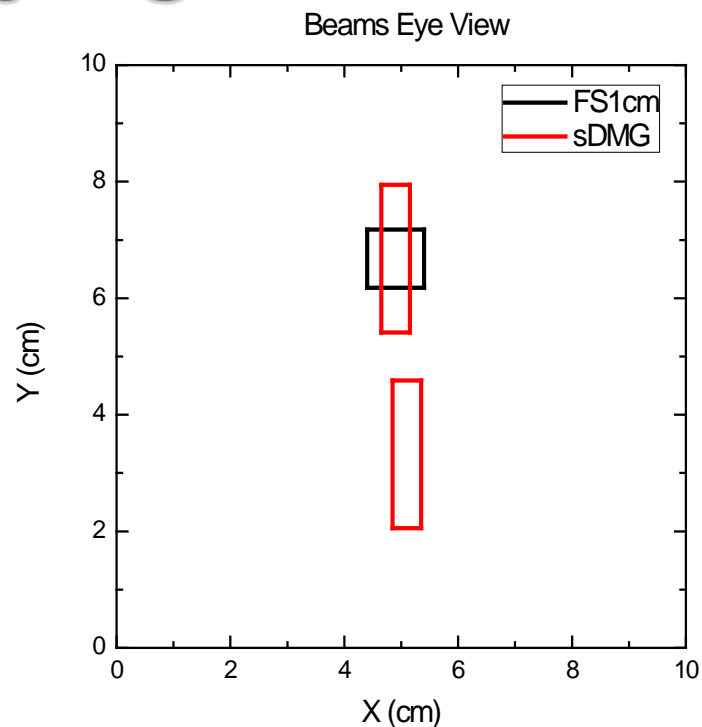
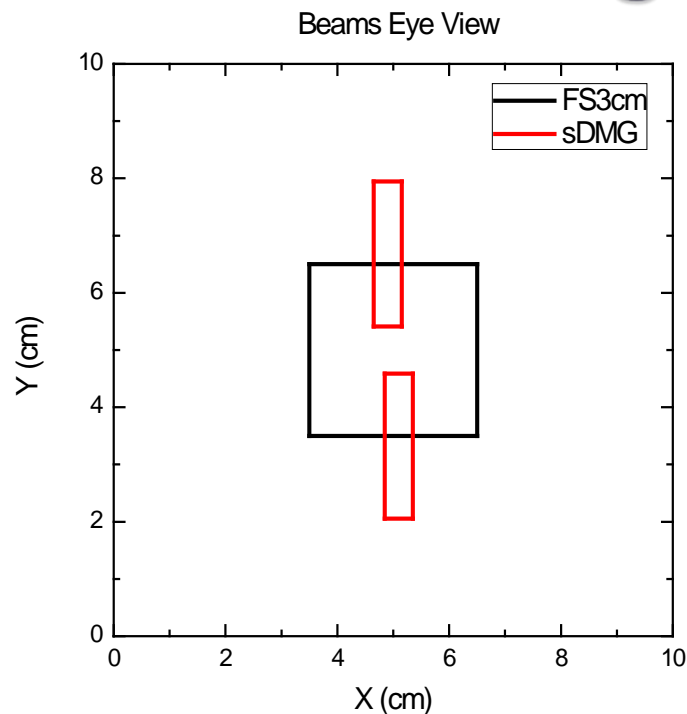


4D image of lung tumour in motion



DMLC tracking of tumour in motion

Serial Dose Magnifying Glass - Setup

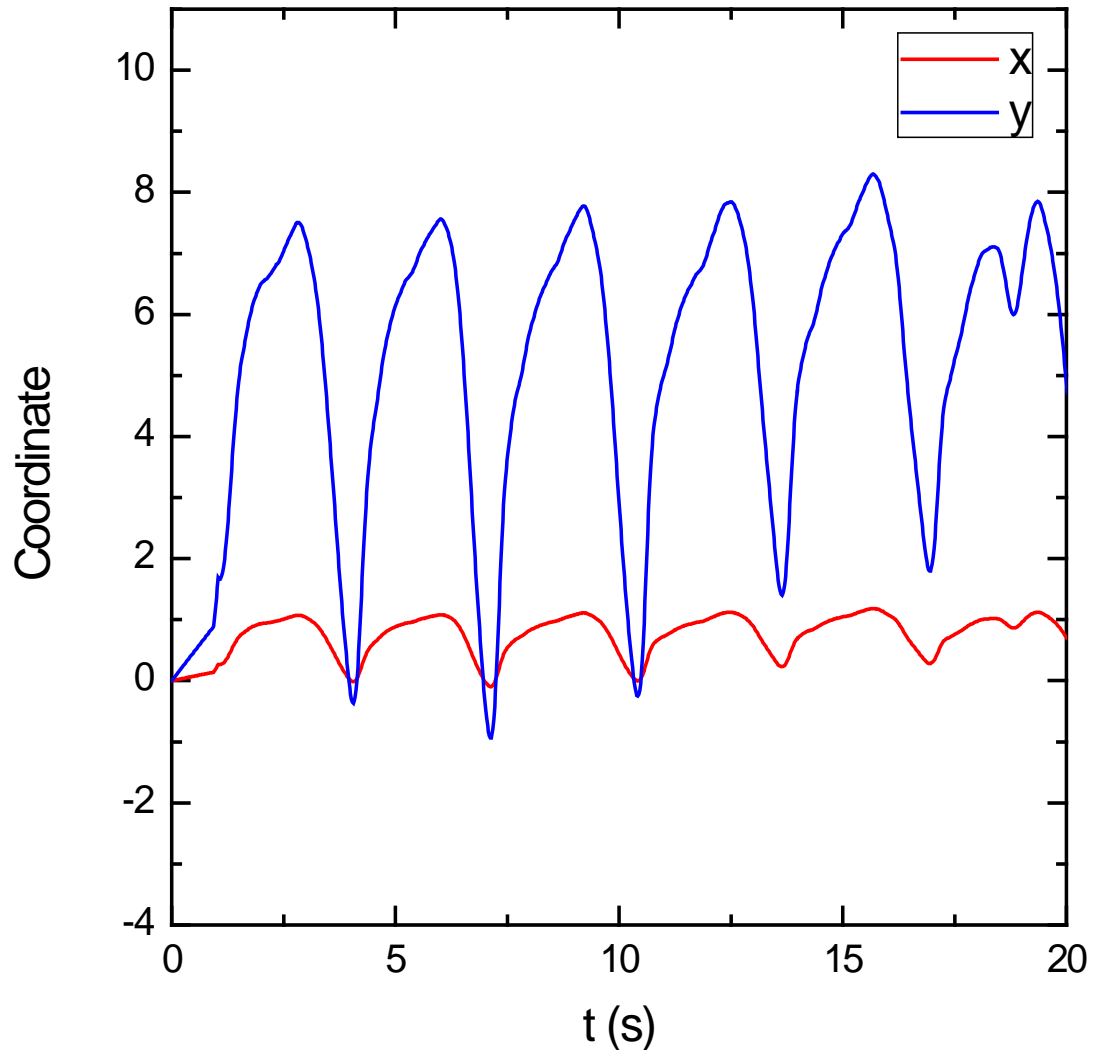


- ▶ Experimental setup geometry illustrated for sDMG measurements.
- ▶ Beam aligned between detector chips to acquire penumbral region for 3x3cm² field size.
- ▶ For 1x1cm² field size, the beam is aligned to the centre of a single detector chip.

Motion – Clinical Lung Trace

x-y coordinates Clinical Lung Trace

- ▶ Clinical lung trace generated by Varian Calypso Motion Tracking system.
- ▶ Motion in x & y coordinates only



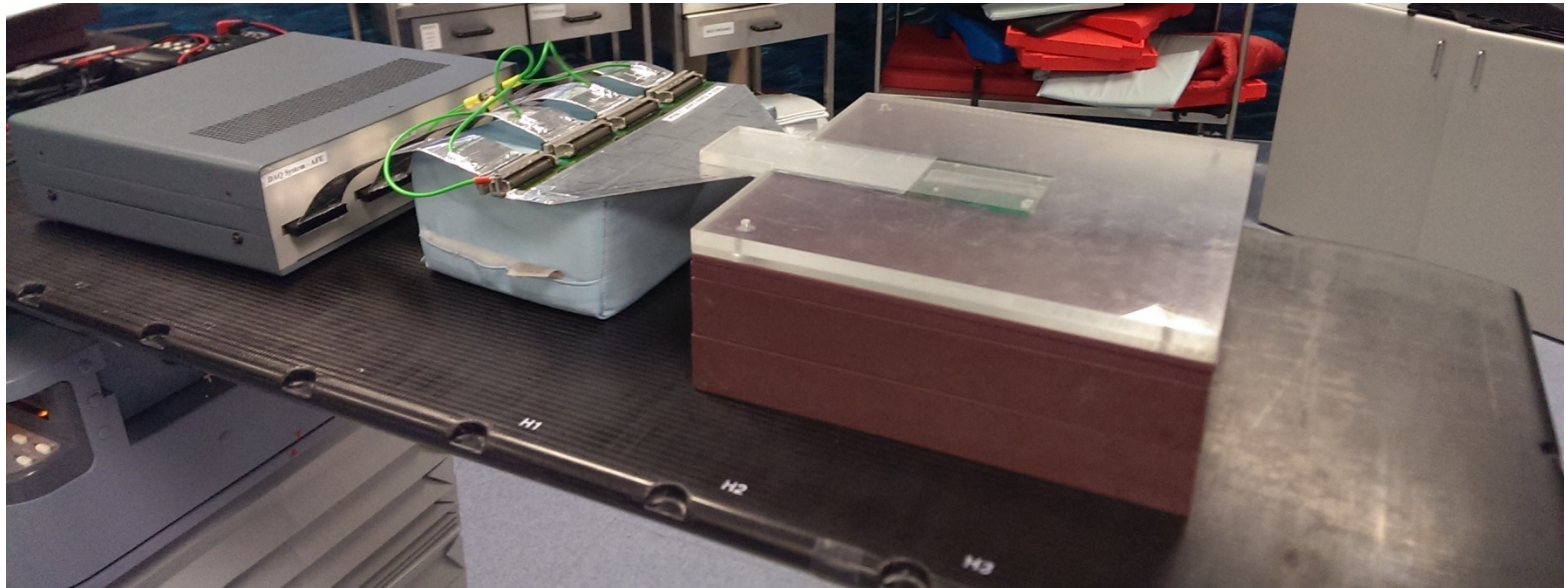
Royal North Shore Hospital (RNSH)

- ▶ MagicPlate 512 (MP512) or sDMG placed upon Scandidos Hexamotion movable phantom.
- ▶ Lung motion pattern from 4D CT lung library



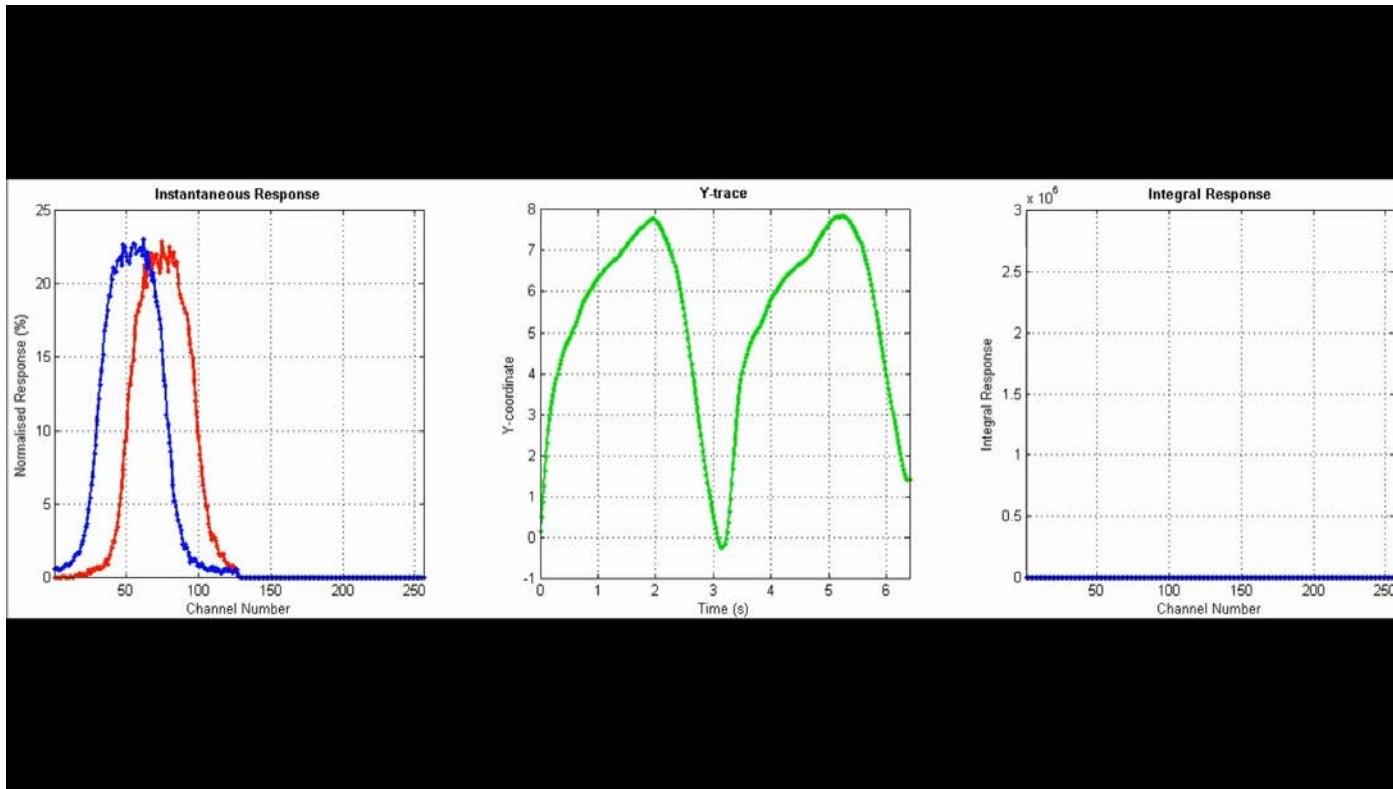
MP512 - sDMG

- ▶ AFE data acquisition (DAQ) system.
- ▶ The acquisition of data by the system is triggered; **integration dose pulse-by-dose pulse.**



– sDMG in a phantom and connected to DAQ QA placed on a LINAC couch .

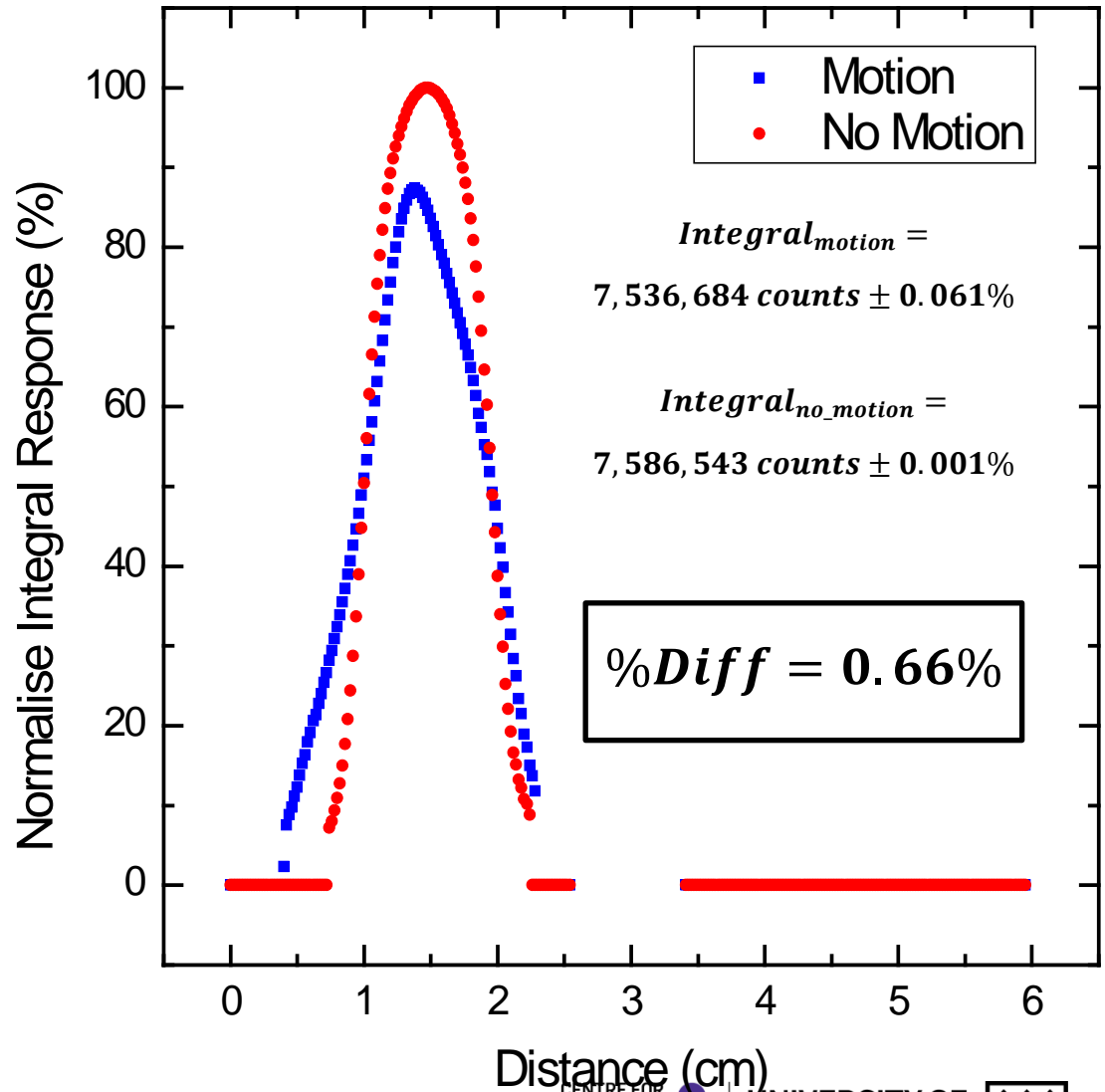
sDMG Measurement – 1x1cm² Field Size



- ▶ 'Motion' and 'No Motion' measurements are shown.
- ▶ Illustrating the instantaneous and cumulative effects of clinical lung motion upon the position of a 1x1cm² beam.
- ▶ 'Clinical Lung Trace' loaded into Hexamotion phantom and engaged for single acquisition of 'Motion' data.

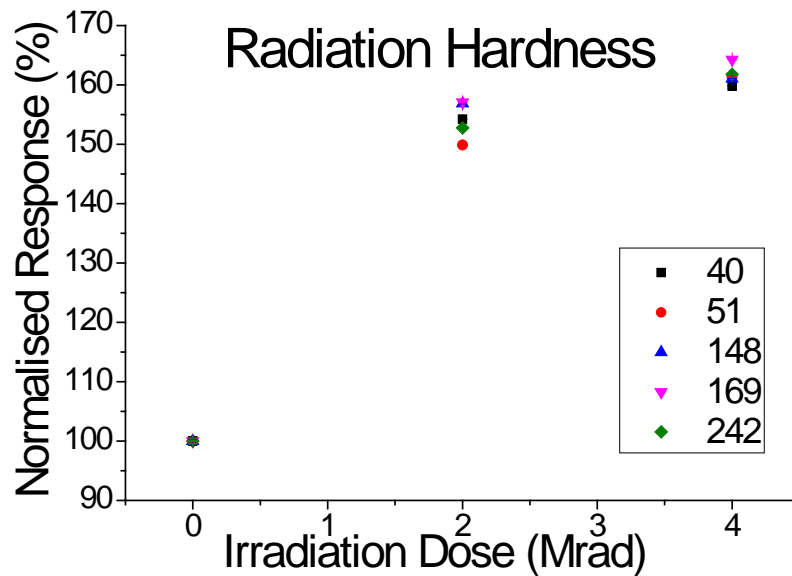
sDMG Measurement – 1x1cm² Field Size

- ▶ sDMG placed at 1.5cm depth in solid water upon Hexamotion phantom and aligned to single DMG detector.
- ▶ Acquisition of 200MU of 1x1cm² beam repeated with and without motion supplied by phantom.
- ▶ Numerical investigation of integral dose measured by detector yields **0.66%** difference between area under 'Motion' and 'No Motion' curves.

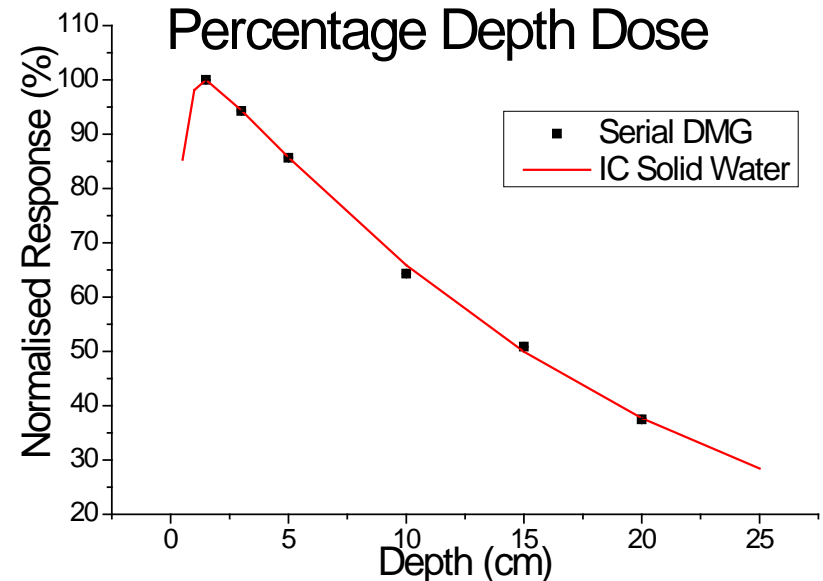


Preliminary Results - sDMG

- ▶ Conducted radiation hardness testing and percentage depth dose measurements.



Radiation hardness study results

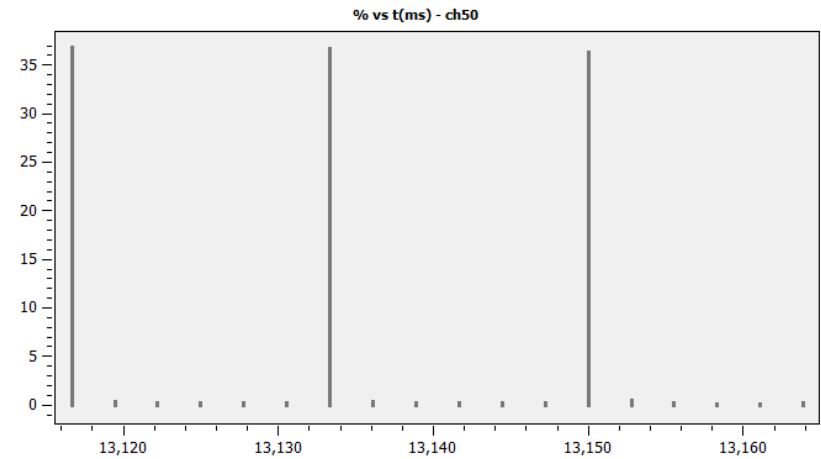
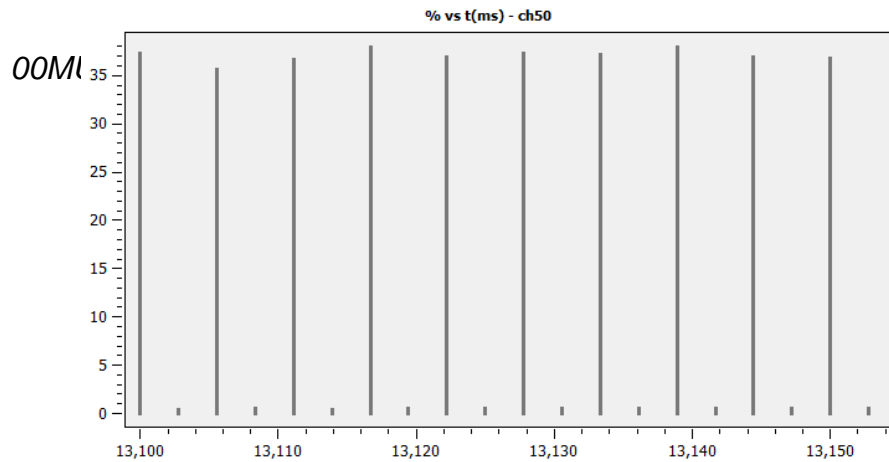
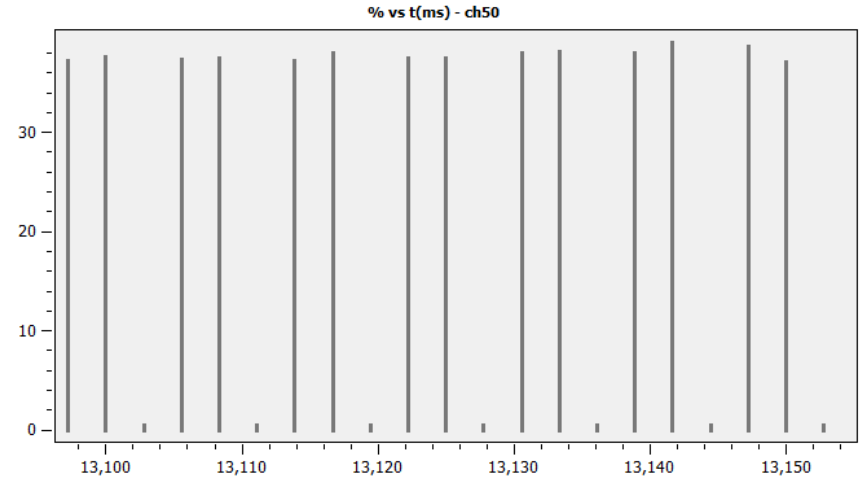
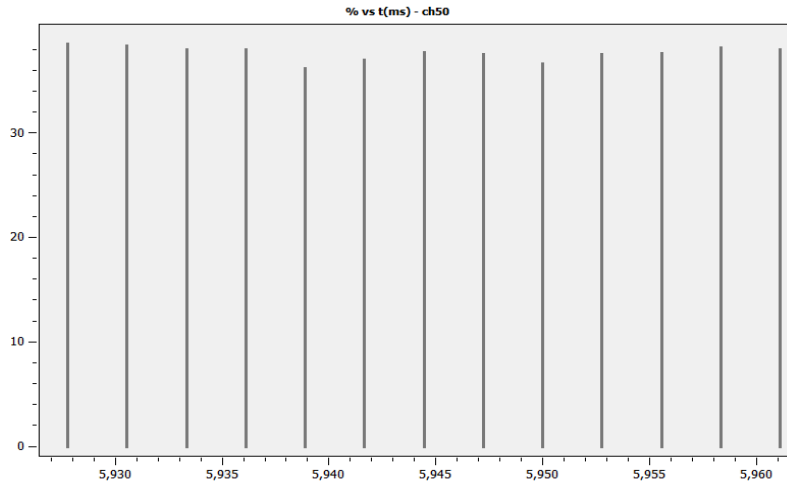


PDD results for sDMG.

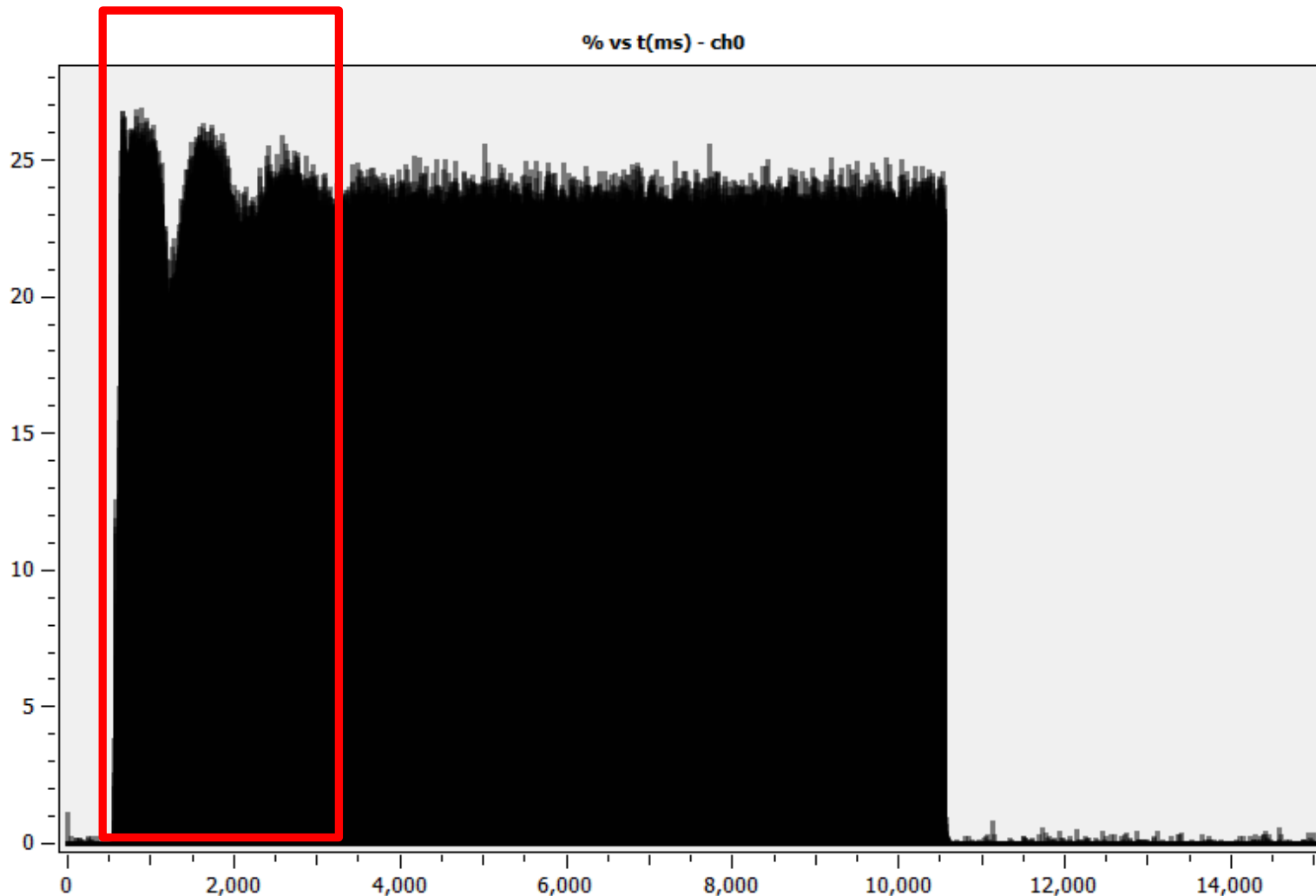
Dose Rate QA in VMAT

600MU/min

00MU/min



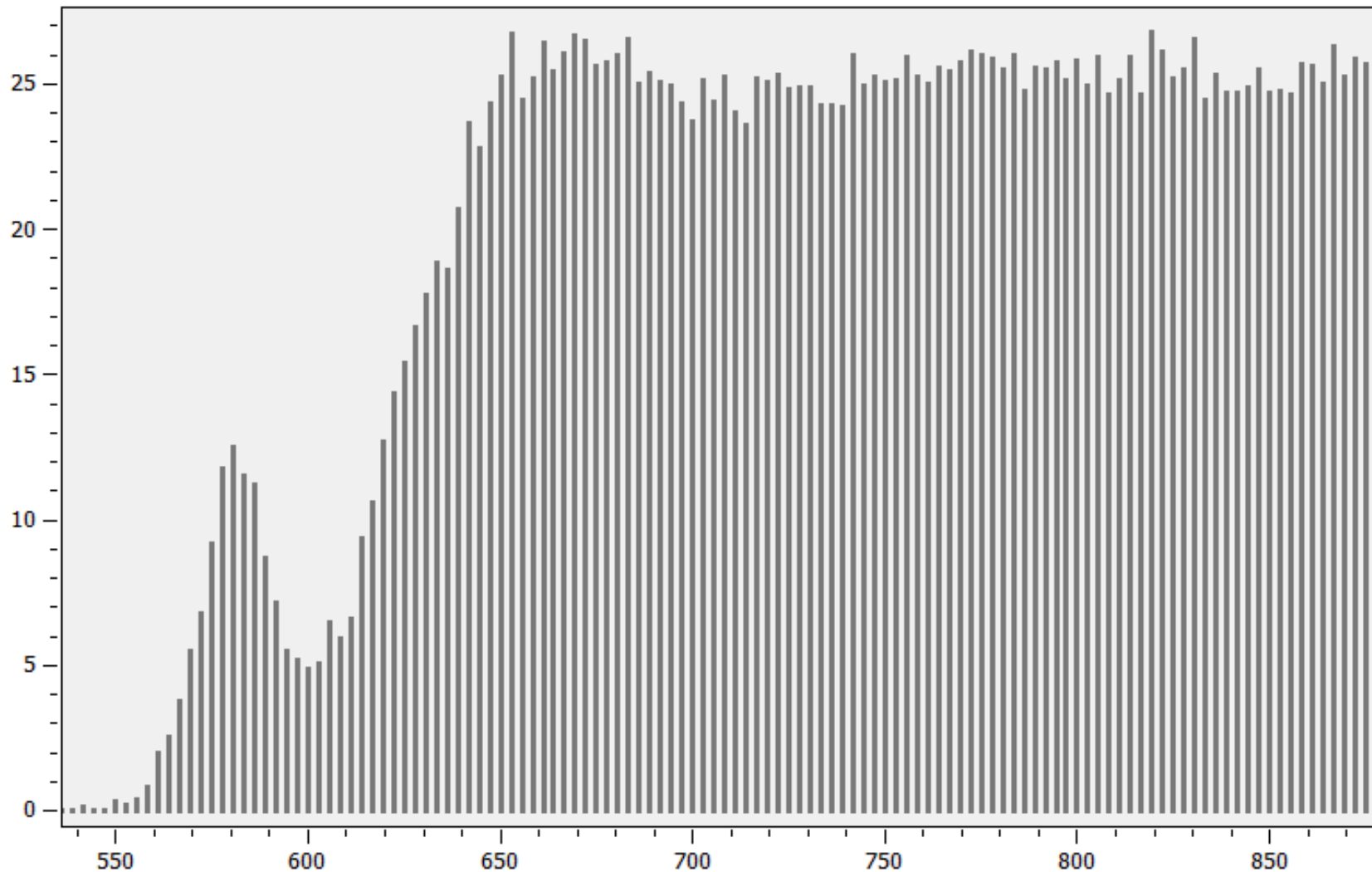
Pulse by pulse DAQ – TI-AFE



Channel 0 response visualised as a function of time after acquisition.

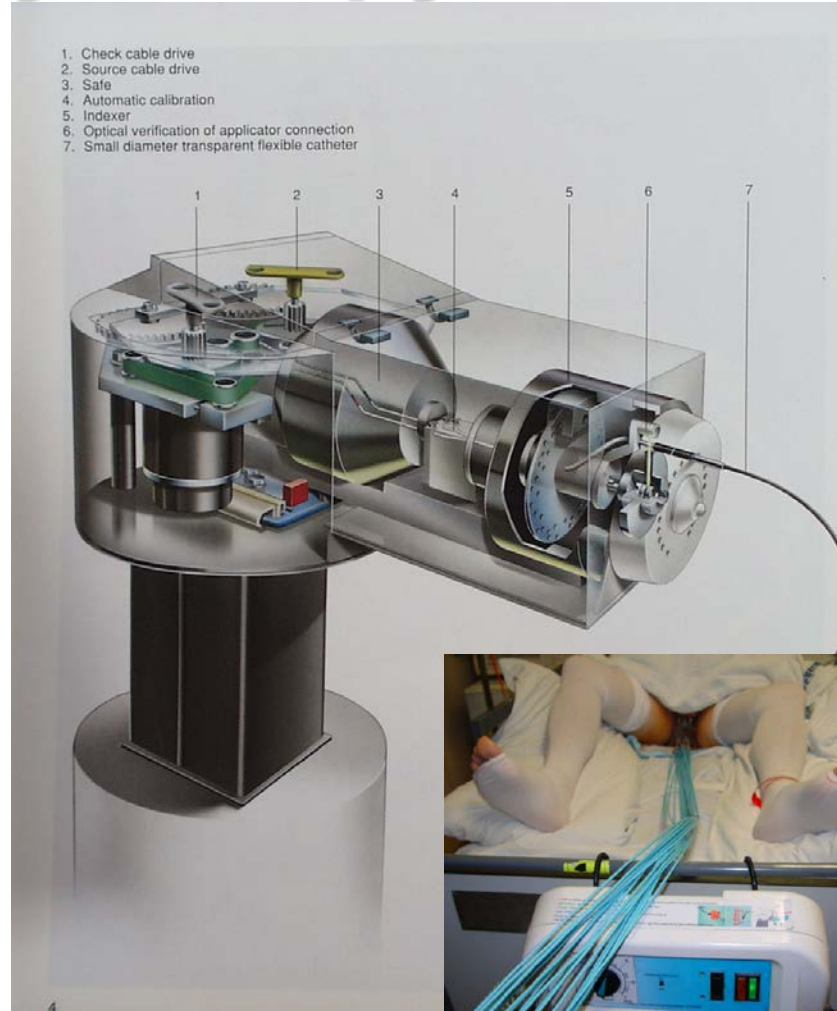
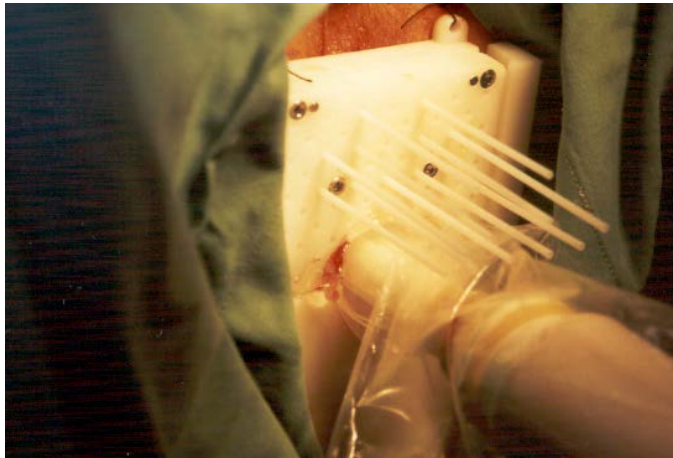
Transient characteristic of individual LINAC

% vs t(ms) - ch0



Zoomed in Channel 0 response visualised as a function of time after acquisition. .

High Dose Rate (HDR) Brachytherapy

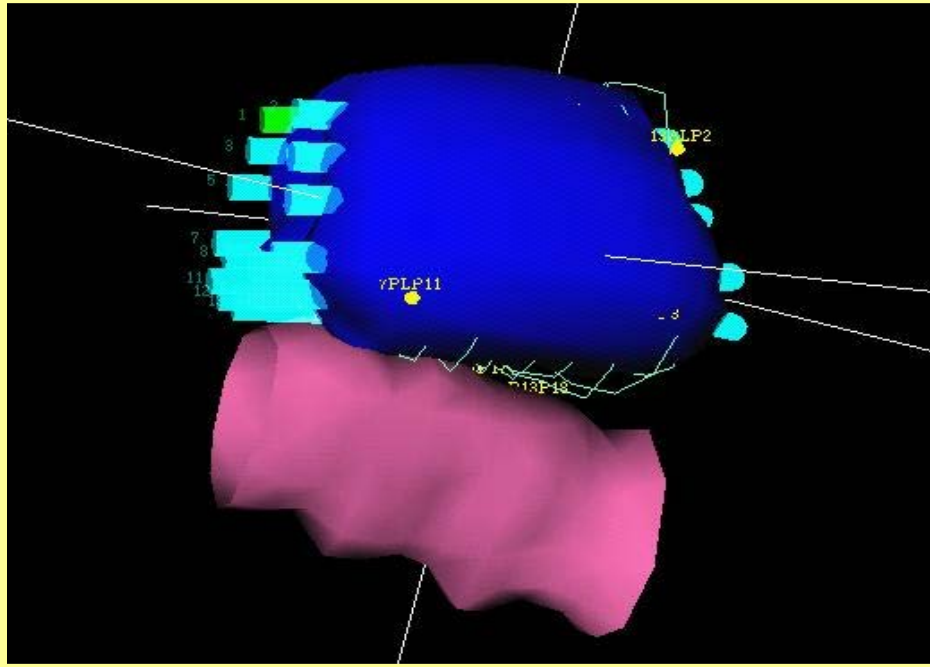


Accidents in High Dose Rate (HDR) Brachytherapy

- ▶ The ICRP publication 97 states that *“More than 500 HDR accidents (including one death) have been reported along the entire chain of procedures from source packing to delivery of dose... many accidents could have been prevented if staff had had functional monitoring equipment and paid attention to the results.”*
(2011)



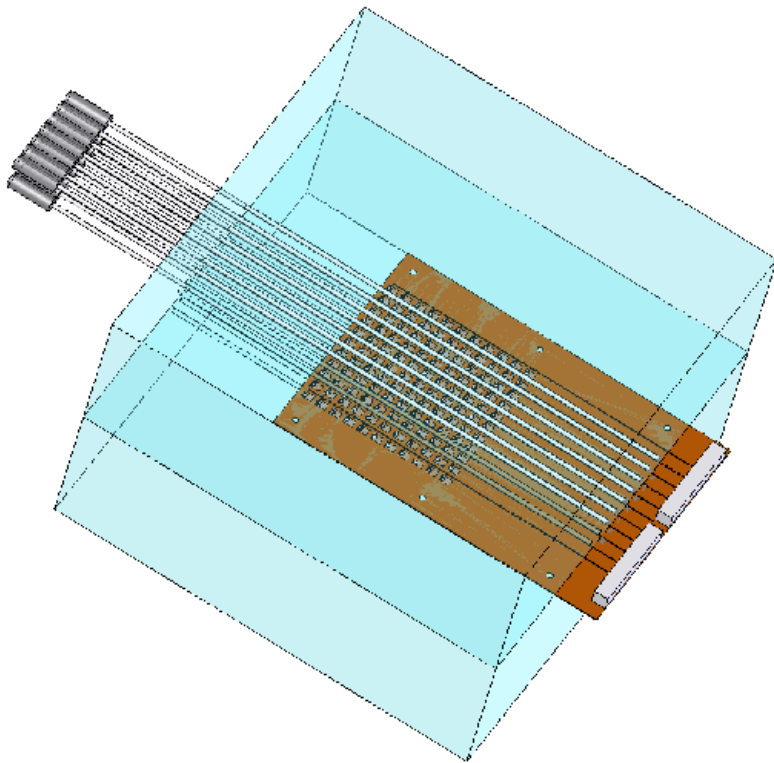
HDR Brachytherapy Quality Assurance



- ▶ Treatment Plan consists of:
 - Patient Geometries
 - Dose at relevant points
 - Catheters for treatment
 - Dwell Positions
 - Dwell Times

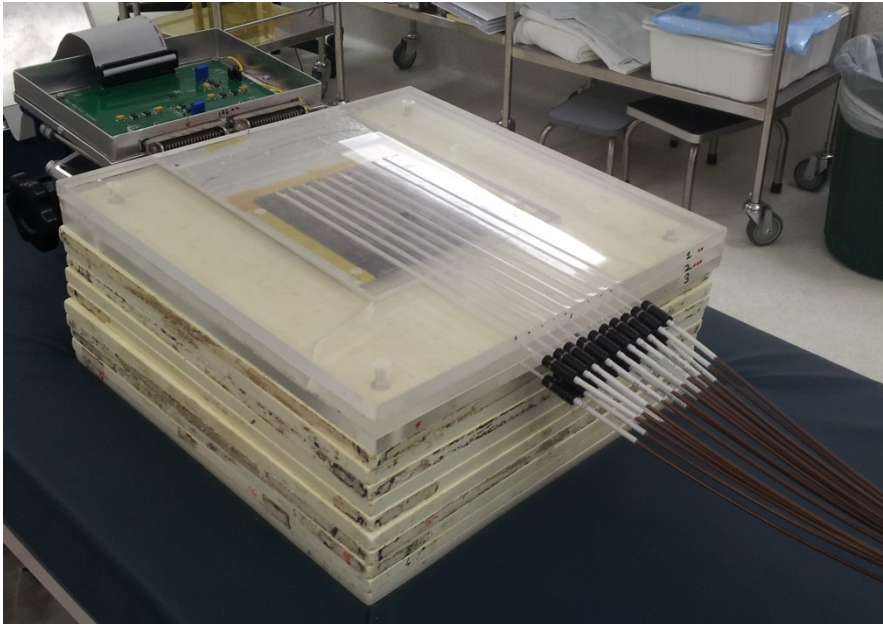
- ▶ Impossible to test every plan with its own system, but with a generic system of fixed geometry and catheter position, possible to assess treatment parameters

Magic Plate - Brachy*Pix* Concept



- ▶ Reconstruction of dose planned from TPS onto the CMRP *Smart Phantom* - Magic Plate sandwiched between planar HDR catheters within solid water
- ▶ Real time error analysis of: timing pattern of source dwellings, source positions and total dose based on detector response
- ▶ Pre-treatment Quality Assurance of HDR afterloader + In-vivo evaluation

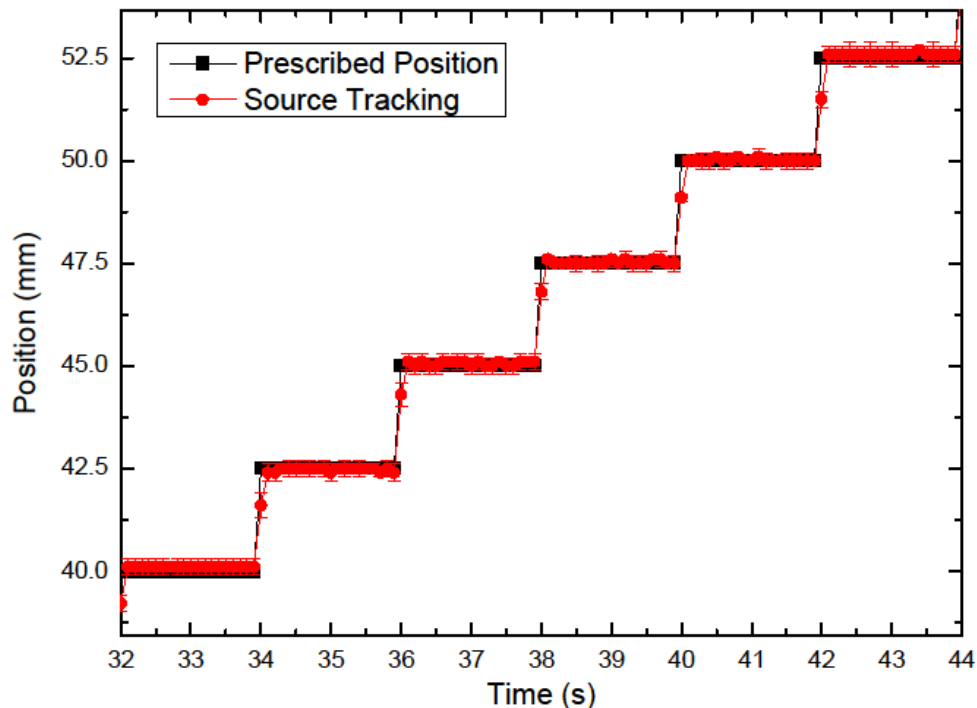
Brachy*Pix* Smart Phantom



- ▶ Portable Brachy*Pix* phantom
 - Three 30x30x1 cm³ Perspex slabs screwed together.
- ▶ Top and bottom slabs have grooves for up to 10 catheters each.
- ▶ Magic Plate inserted within middle slab.
- ▶ 13.5 cm solid water placed on both sides of Brachy*Pix*.
 - Full scattering conditions.

Results - Source Positioning

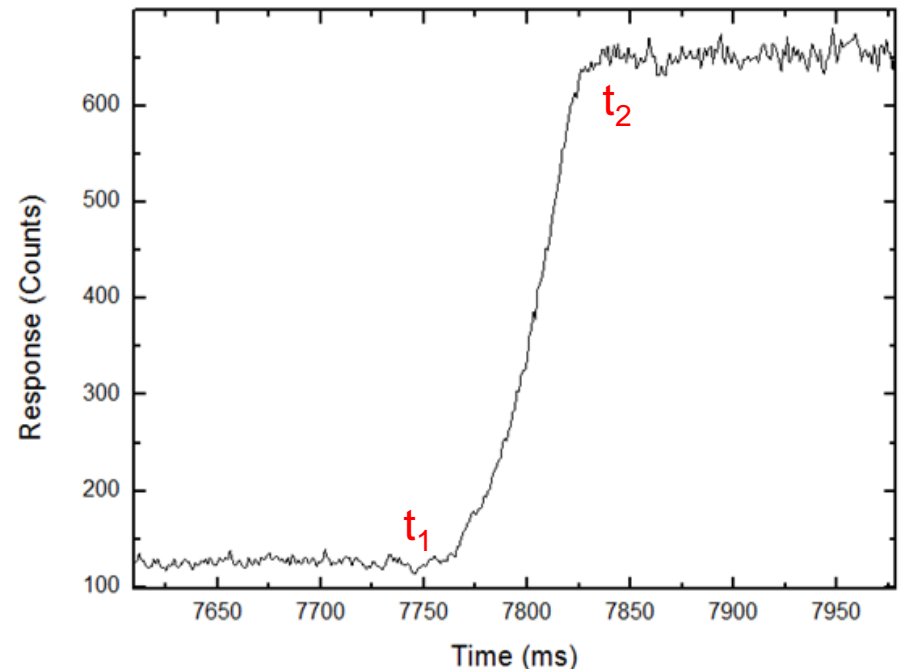
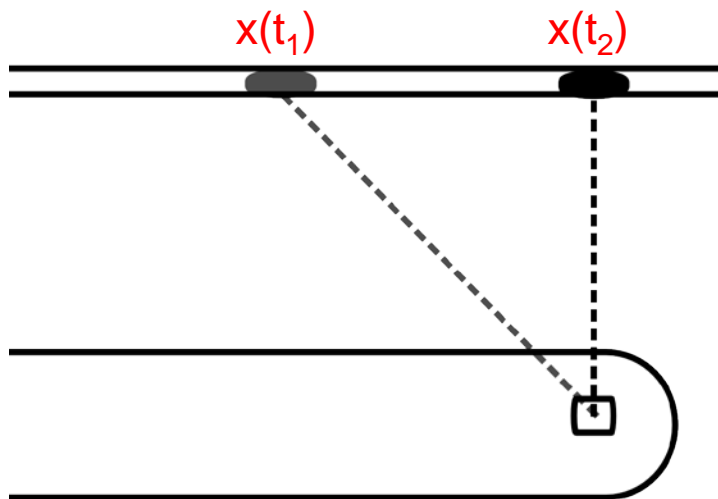
- ▶ Experimental – Magic Plate at depth 6 mm from source within solid water, source steps in at 2.5 mm step sizes, dwell time 2 seconds.
- ▶ Differences in calculated and expected positions are no more than 0.3 mm. Errors are based on two standard deviations and are seen to be a maximum of 0.8 mm, but an average of 0.3 mm. Variations with depths up to 30 mm have seen to be no more than 1 mm.
- ▶ Dwell times are all measured to be 2 seconds.



HDR Average Speed Measurement

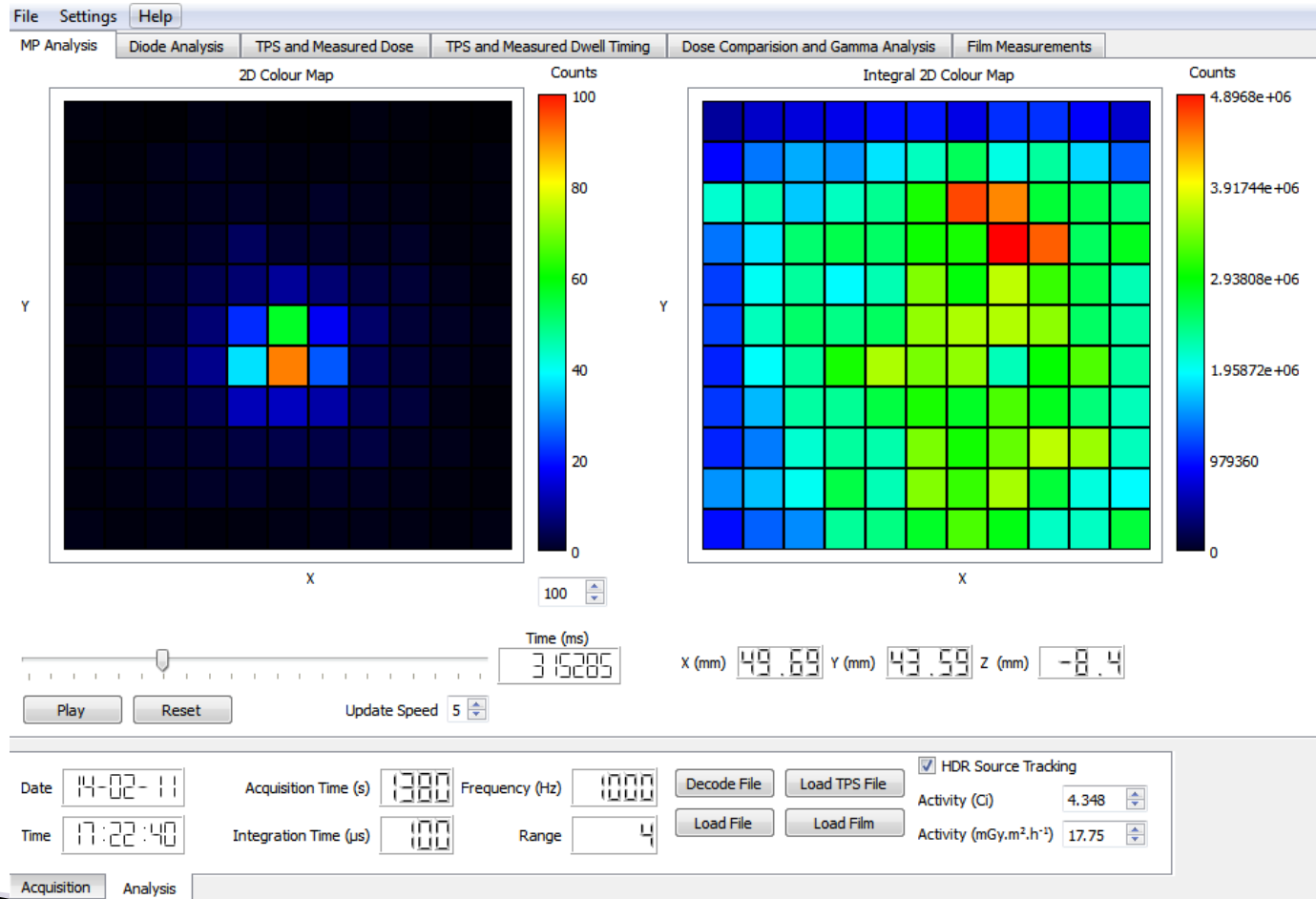
- ▶ The HDR source moves extremely fast between dwell points (~ 50 cm/s) to minimise dose delivered while the source is in transit.
- ▶ Using the CMRP fast electrometer, which can measure the charge generated within the diode at 1 MHz, it is possible to estimate the average speed of the HDR source at varying dwell distances.

N14-195 Poster

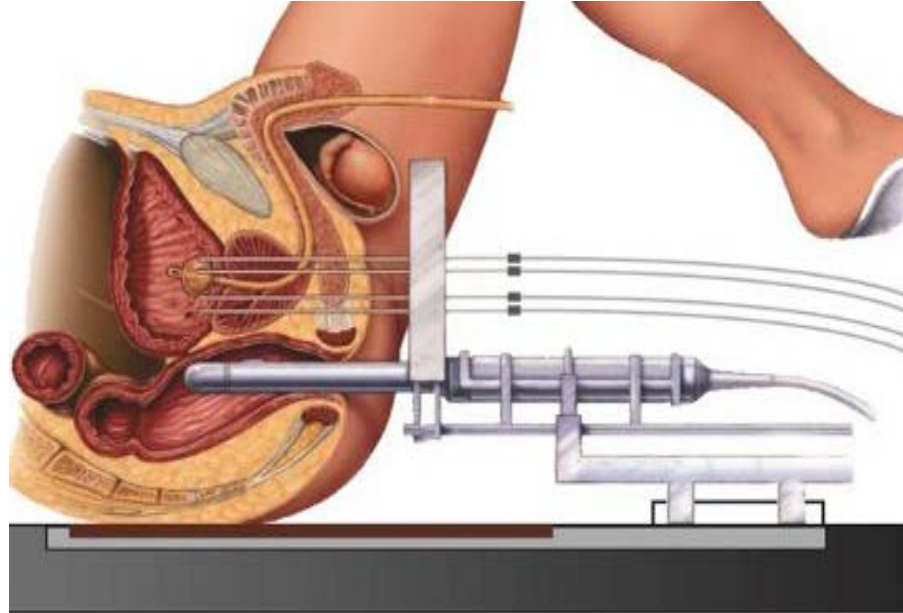


BrachyPix software toolkit

- ▶ C++ software has been developed for BrachyPix. It is capable of:
 - Performing the full measurement and saving for later viewing.
 - Full plan analysis of dwell positions and dwell times



In Vivo QA in HDR brachytherapy



BMP512 is embed in a couch and placed below prostate. TRUS probe stepper frame is fixed on a couch making rigid alignment with a BMP512.

Conclusions

- ▶ Dual purpose MP Detector array
- ▶ Demonstrated ability to verify IMRT dose
 - In phantom
 - In transmission mode
- ▶ On going/future development –
 - Monte Carlo simulation to predict transmission mode signal.
 - Inclinator - real time angular information
 - FPGA-USB readout system
- ▶ New prototype has 512 detectors



MEDIPIX in Radiation Therapy

QA

CENTRE FOR
MEDICAL
RADIATION PHYSICS



UNIVERSITY OF
WOLLONGONG



BrachyView : QA Concept in RT

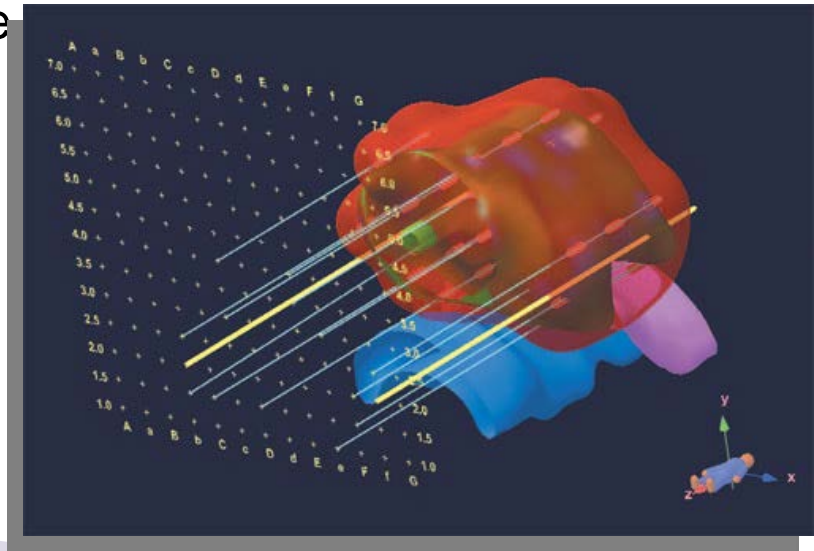
Firstly introduced and patented by CMRP

In Body Imaging

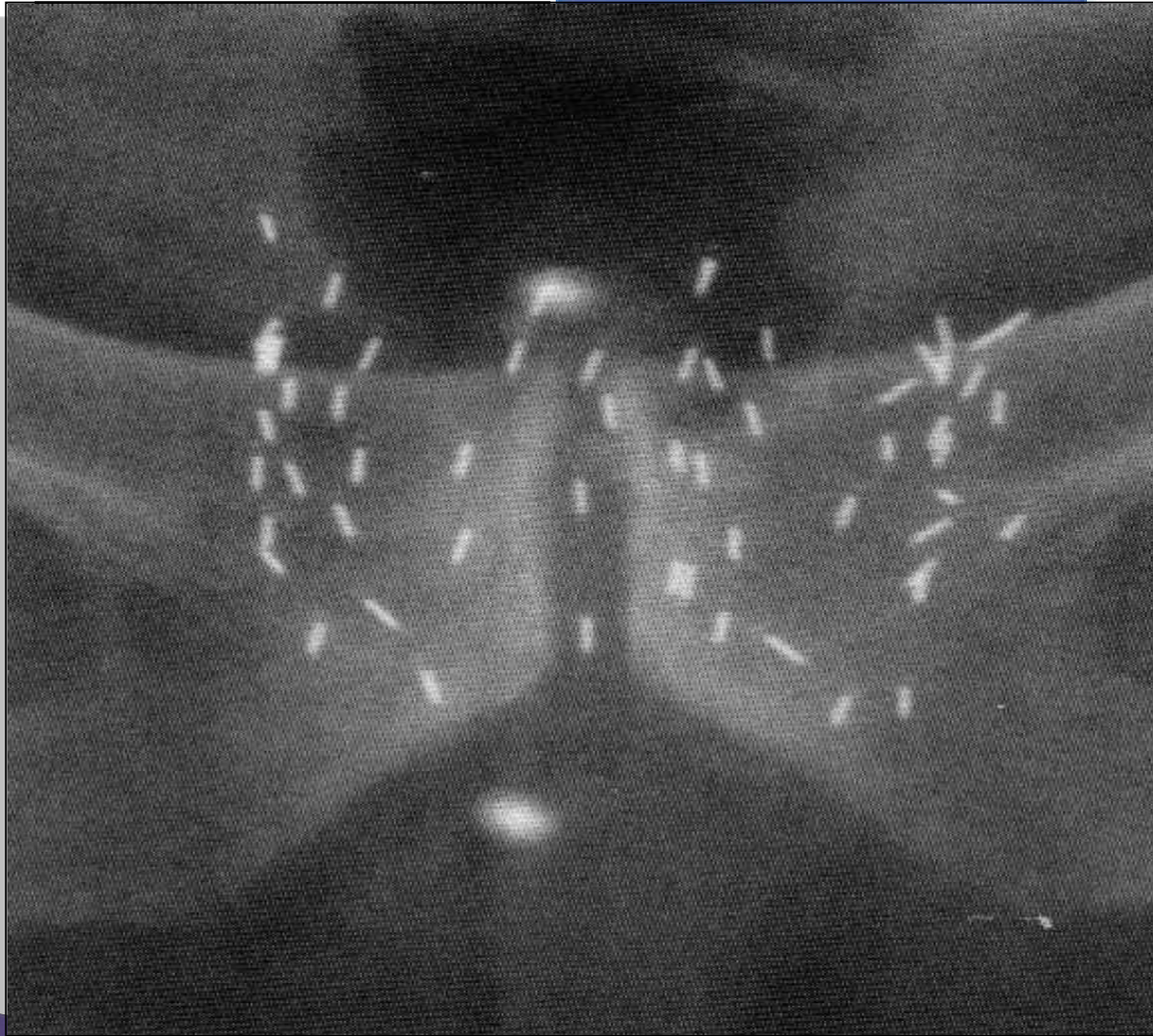
for advanced QA in brachytherapy for prostate cancer treatment

Concept

- ▶ Seed localisation uncertainty causes dosimetric complications
 - Prostate mobility
 - Seed twisting
 - Brachy needle placement errors
- ▶ Intraoperative dynamic dose planning
 - Fuse with existing ultrasound technology
- ▶ New in-body ultra-functional probe:
 - Ultrasound, radiation source and CT imaging captured real-time
 - Possibility to introduce fast, online seed position imaging using seeds themselves as radiation source
- ▶ Applications:
 - Seed positioning in tumour
 - Real-time CT imaging of implants



Current Technology – TRUS



Result

- Seed misplacement errors
- Urethral and rectal toxicity: 40% cases
- No real-time planning option available



Example: C-arm Fluoroscopy

- ▶ Obtain plane image of seeds without positioning relevant to anatomy
- ▶ Similar goal of registering TRUS and fluoroscopic images (technically difficult to perform)
- ▶ *Post-implant dosimetry*: impossible to change seed position
- ▶ **Disadvantage**: not true 'real-time', planar image only (no anatomy), cumbersome and expensive equipment

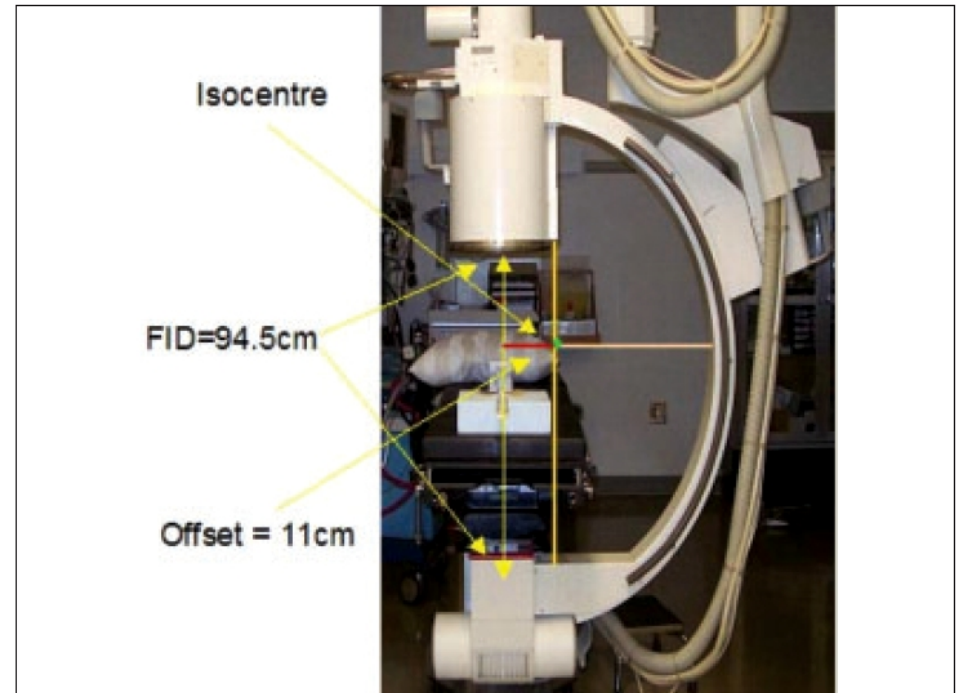


Figure 1: C-arm X-ray unit used in the study, the offset between the position of the centre of rotation and the X-ray beam central axis is illustrated. (FID - focus to -image intensifier distance)

Ravindran, Lewis et al 2006

Tomography in PiPB

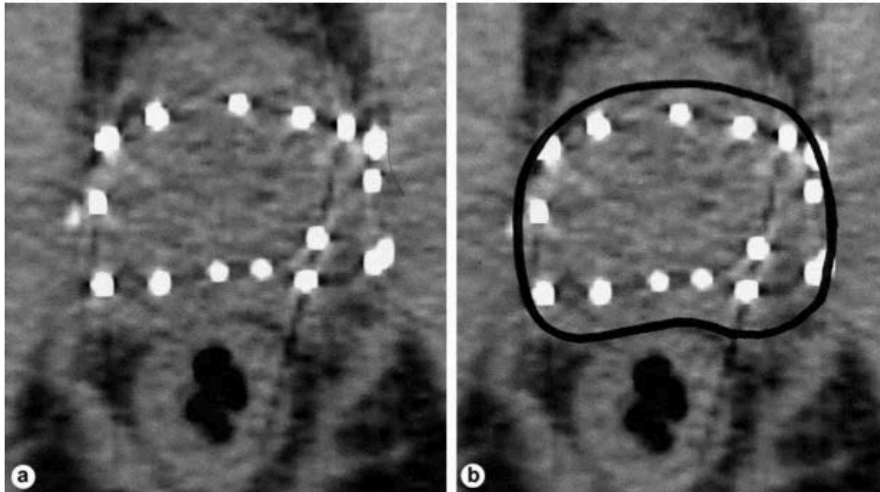


Fig. 1. Transverse CT image of implanted prostate: (a) without contoured prostate; (b) with prostate contour

- ▶ *Because the quality of the procedure postimplantation computed tomographic dosimetric outcomes only become apparent after reviewing the postimplantation CT scan for a flawed implant requires an*

- Zelefsky, 2011

is an essential component of the only method of assessing the prostate and normal surrounding tissue post-implant and continues to improve permanent brachytherapy as an effective treatment for

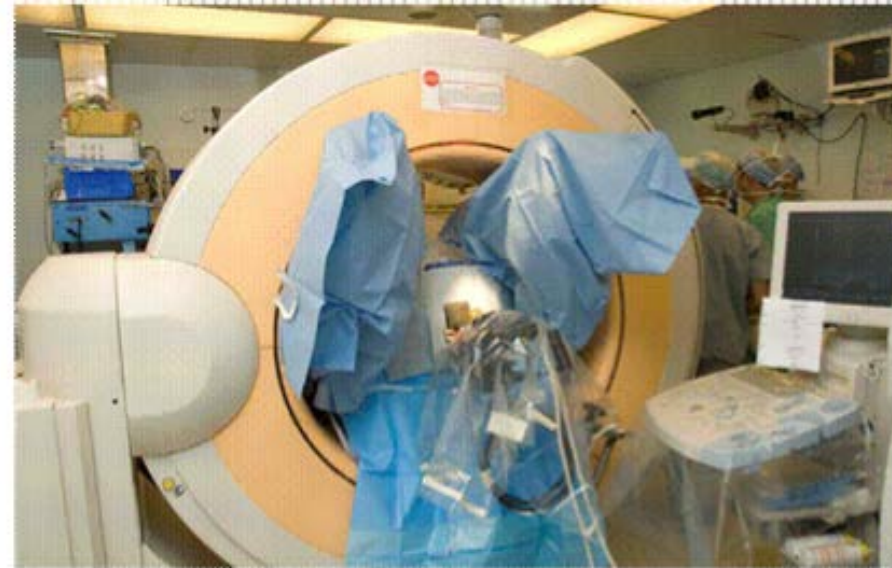
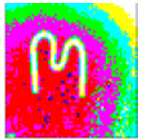


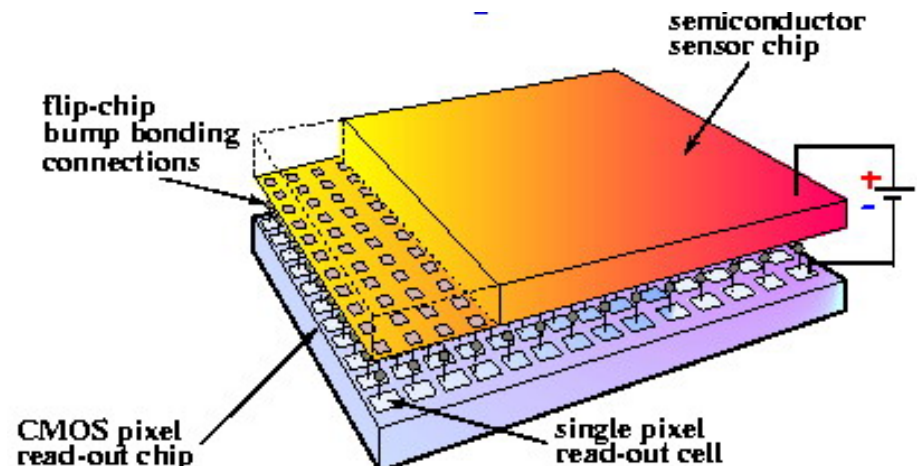
Figure 1. Patient with implanted needles in extended lithotomy position with CBCT imager in place.

Medipix device:

Single particle counting pixel detector

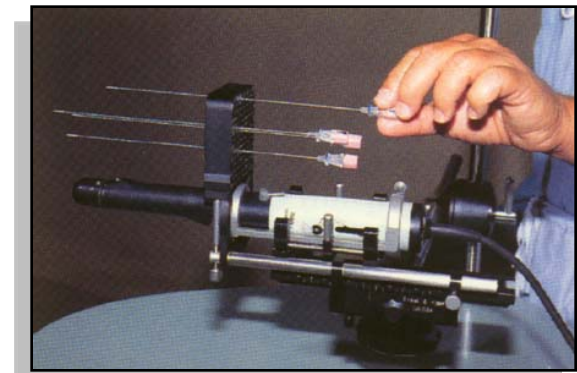
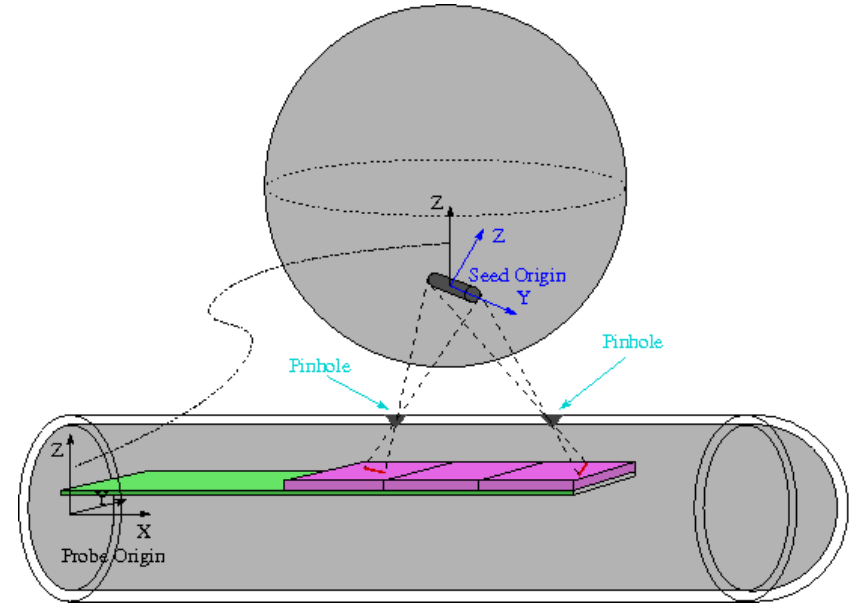


- Planar pixellated detector (Si, GaAs, CdTe, thickness: 300mm)
- Bump-bonded to Medipix readout chip
- Pixels in one single Medipix2: 256 x 256
- Pixel size: 55 x 55 μm^2
- Area: 15 x 15 mm^2



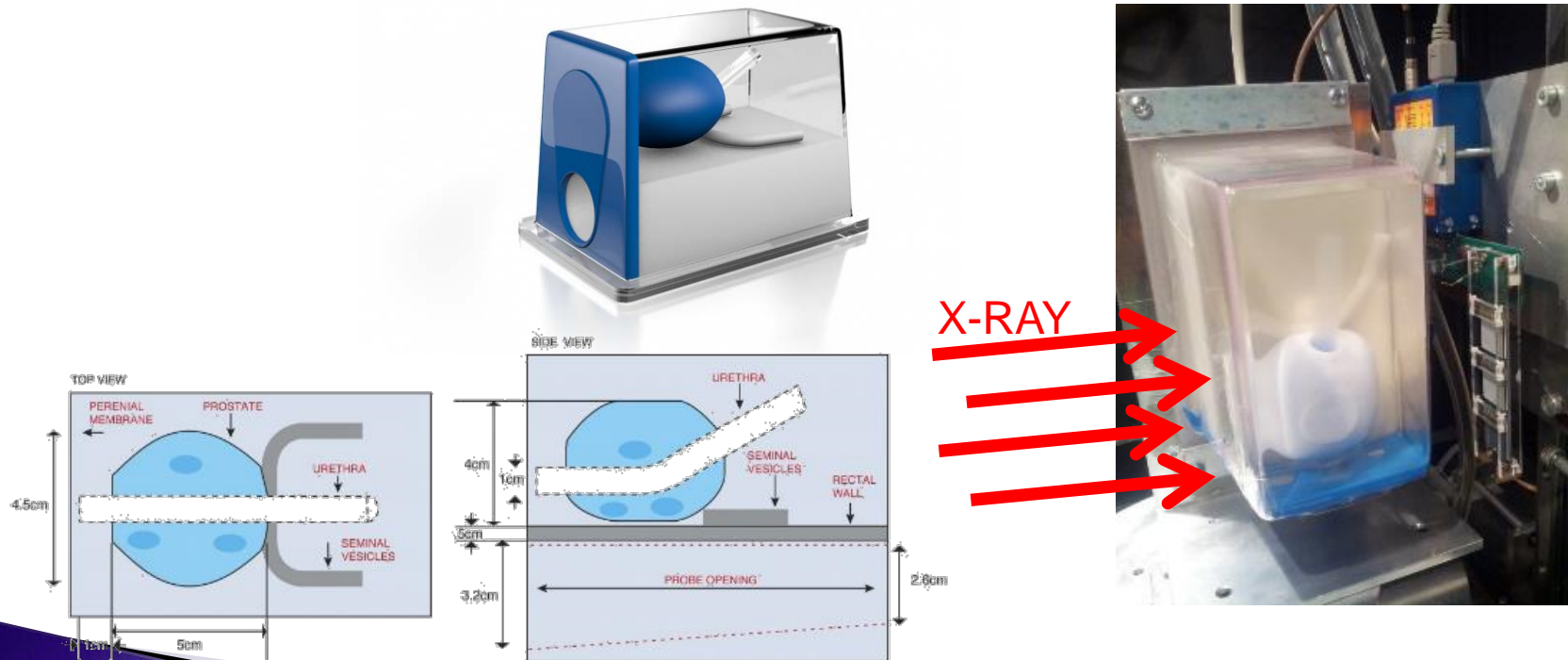
BrachyView: Pinhole Application

- ▶ In-vivo detector plane integrated into TRUS probe
- ▶ Use seeds themselves as source of imaging radiation
- ▶ Seed position reconstruction via 'camera obscura' concept
 - Using lead pinhole collimator, reconstructions have been found to be within 0.5-1mm of expected positions
- ▶ Real-time, intraoperative treatment planning seed positioning possible during implant procedure

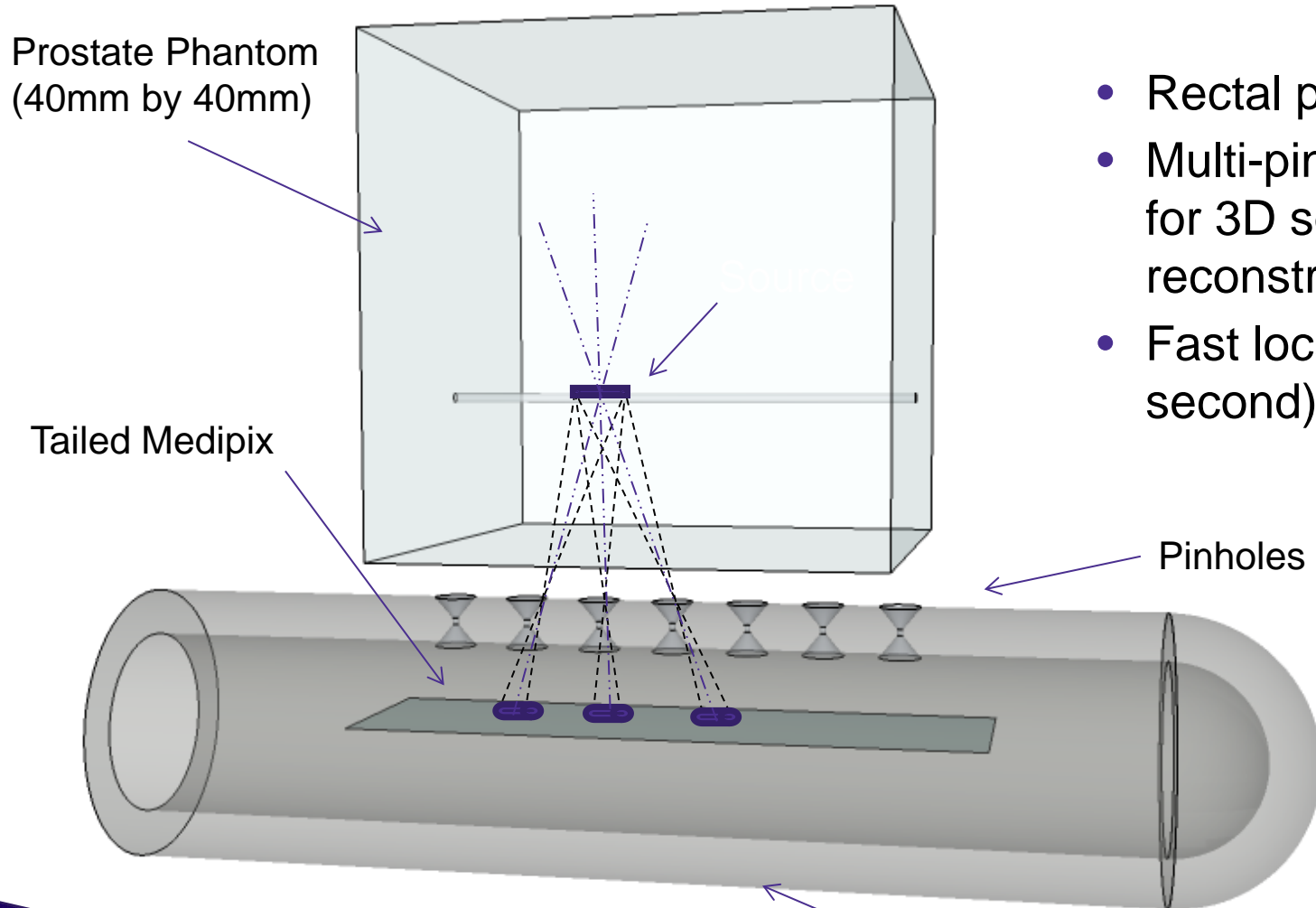


Soft tissue diagnostic imaging

- ▶ Feasibility studies completed to investigate the applicability of TimePix for soft tissue imaging
- ▶ Well-known device for distinguishing materials of similar composition (plexiglass, water, acrylic materials)
- ▶ Delineation of prostate soft tissue, lesions, urethra etc



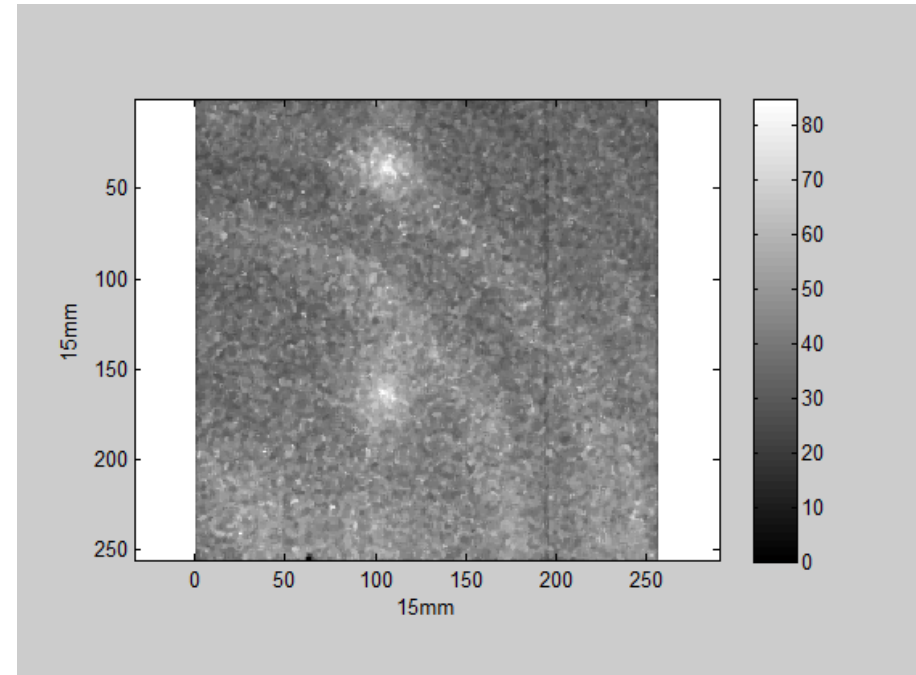
HDR BrachyView Probe: Ir-192 Source Tracking



- Rectal probe
- Multi-pinholes imaging for 3D source position reconstruction
- Fast localization (sub-second)

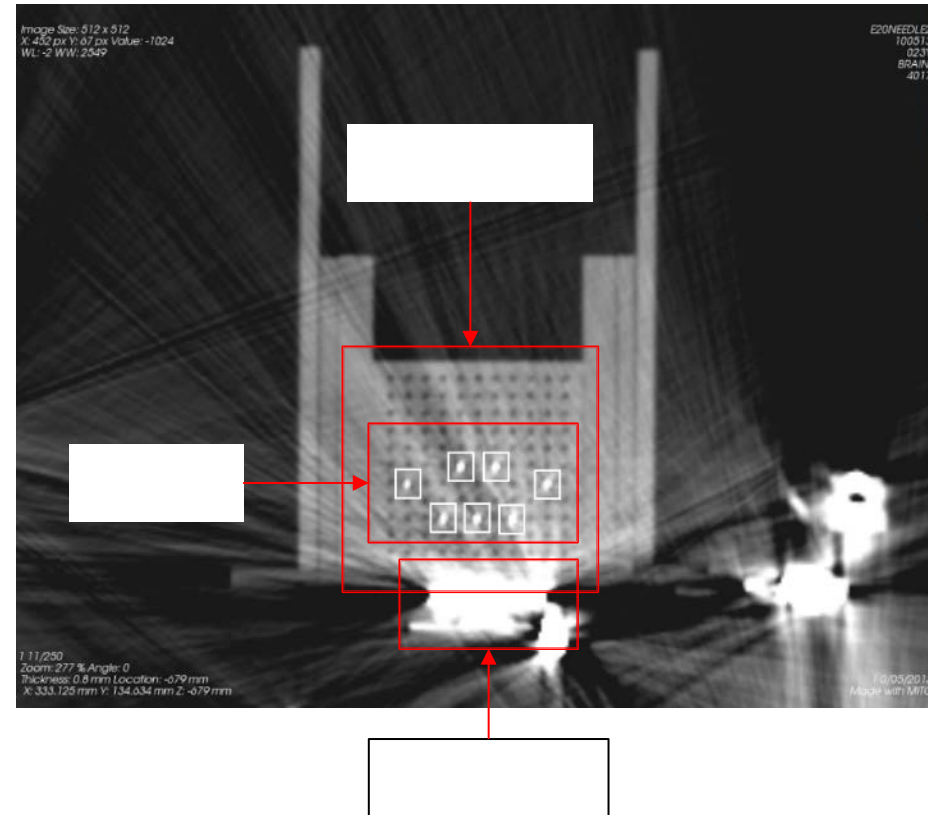
Pinhole imaging Experiment: Result

- Source placed 40mm above the collimator
- Real dwelling time: 1.7s
- Acquisition time: 0.5s/frame
- The video presents every 3 frames



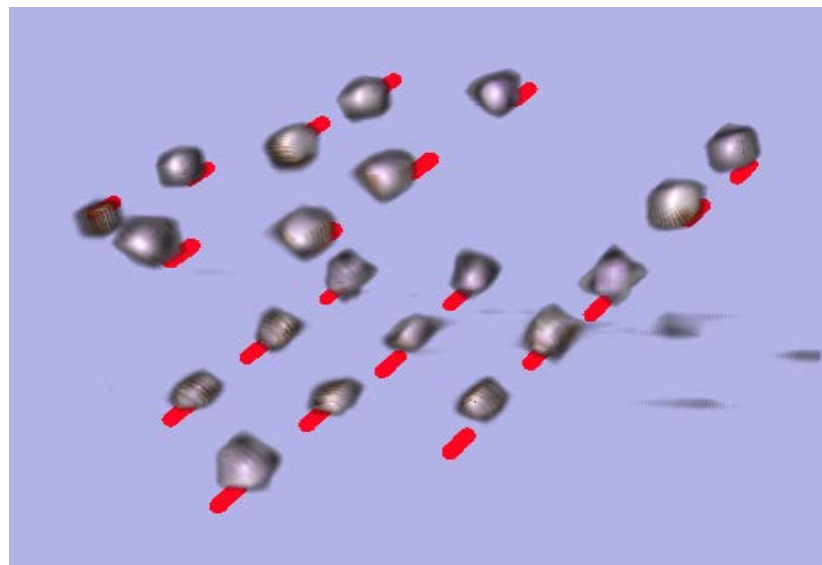
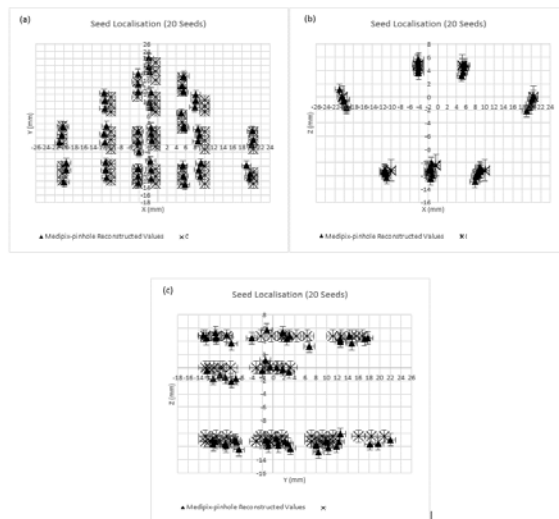
Seeds localisation: CT vs BrachyView

- ▶ Prostate phantom with 20 seeds was scanned on CT
- ▶ Each CT slice corresponds to 0.8 mm thickness, which allowed higher accuracy than the typical 2 mm thick slice used for patients
- ▶ Two datasets:
 1. TimePix 2D maps
 2. Full CT scan as a reference



CT-BrachyView: image fusion

- ▶ Co-register the 3D coordinates to obtain full information for seed location in phantom
- ▶ 3D combined view of CT DICOM and BrachyView in 3DSlicer (standard freeware license software for DICOM visualisation)



3D Silicon Microdosimetry

CENTRE FOR
MEDICAL
RADIATION PHYSICS



UNIVERSITY OF
WOLLONGONG



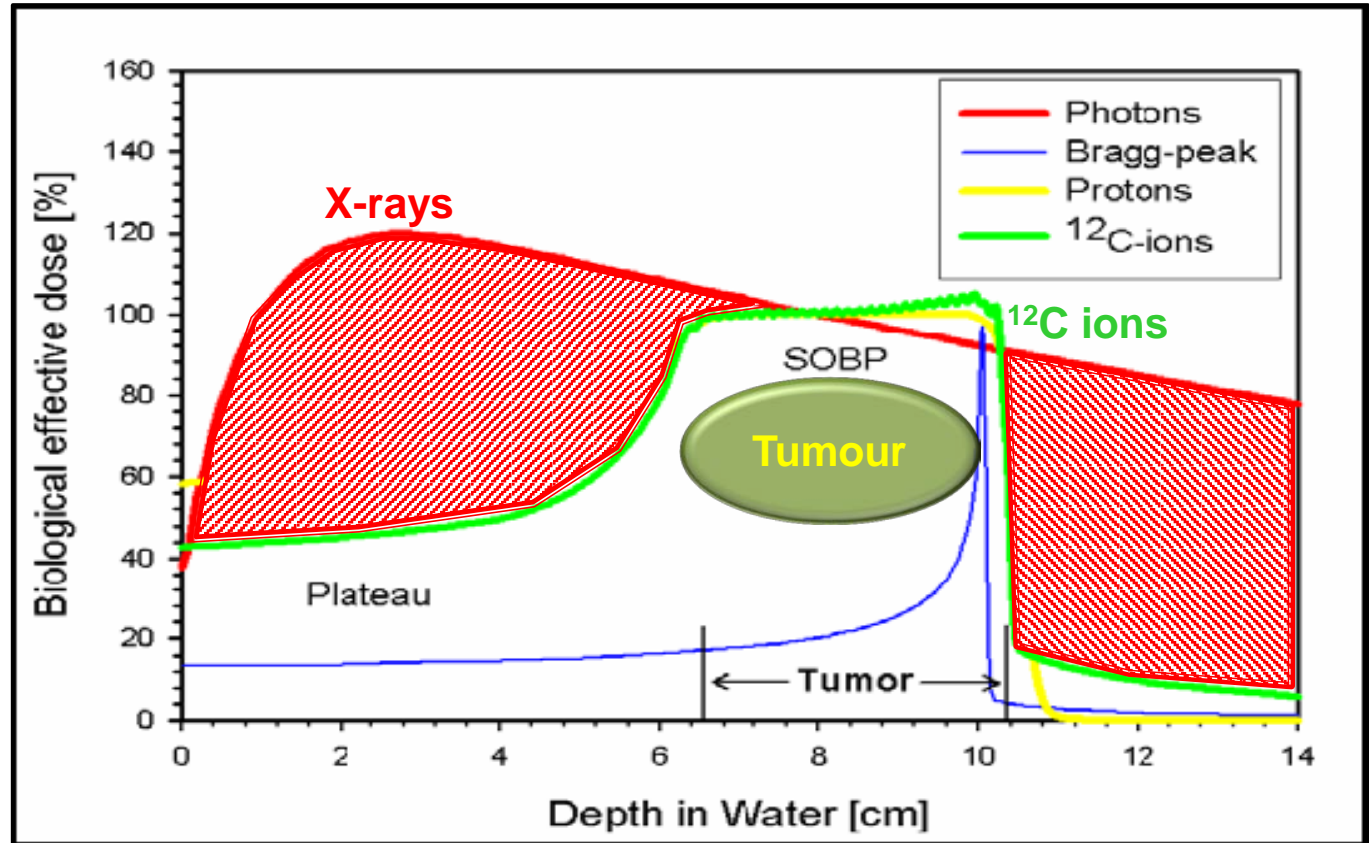
Proton and Heavy Ion Therapy

Protons & carbon
Bethe Formula
Dose conforma

$$-\frac{dE}{dx} = \frac{4\pi}{m_e c^2} \cdot \frac{nz^2}{\beta^2} \cdot \left(\frac{e^2}{4\pi\epsilon_0}\right)^2 \cdot \left[\ln\left(\frac{2m_e c^2 \beta^2}{I \cdot (1 - \beta^2)}\right) - \beta^2 \right]$$

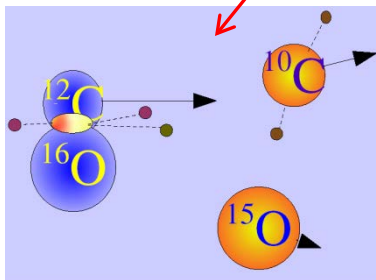
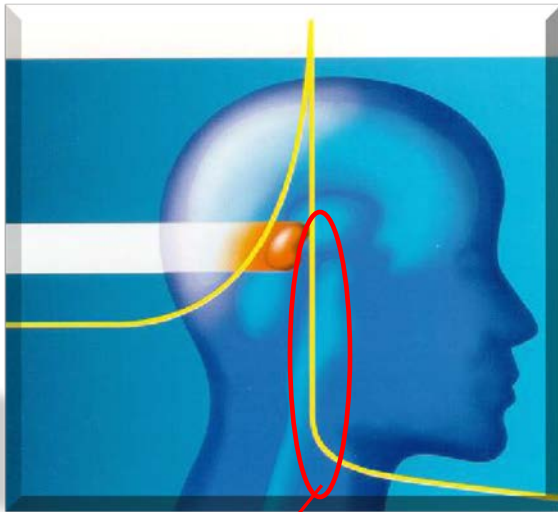
The cancerous tumors are removed most efficiently by the ion radiation as it had been previously (1946) recognized by R. Wilson.

[Radiological use of fast protons. Radiology 47:487-91, 1946].

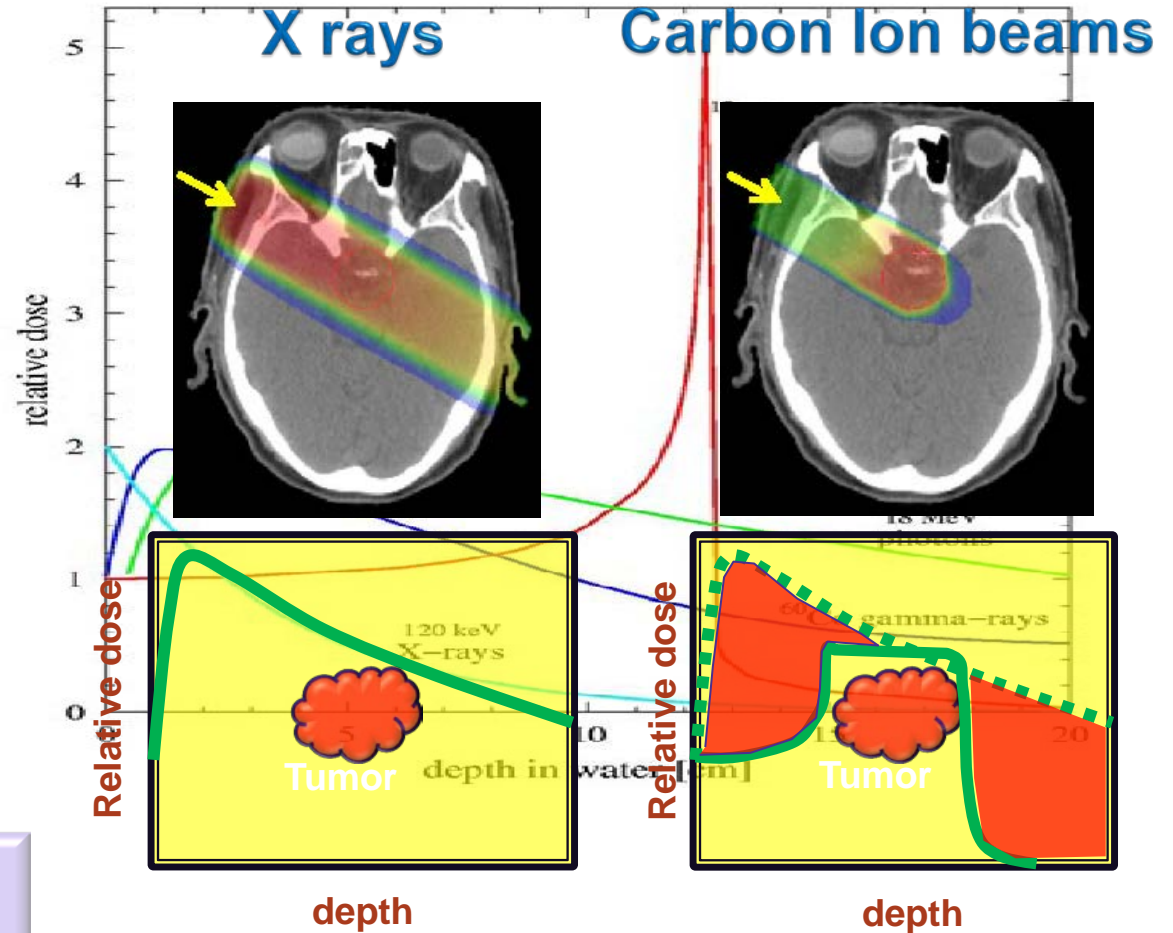


Different: **biological effectiveness**

Heavy Ion Therapy

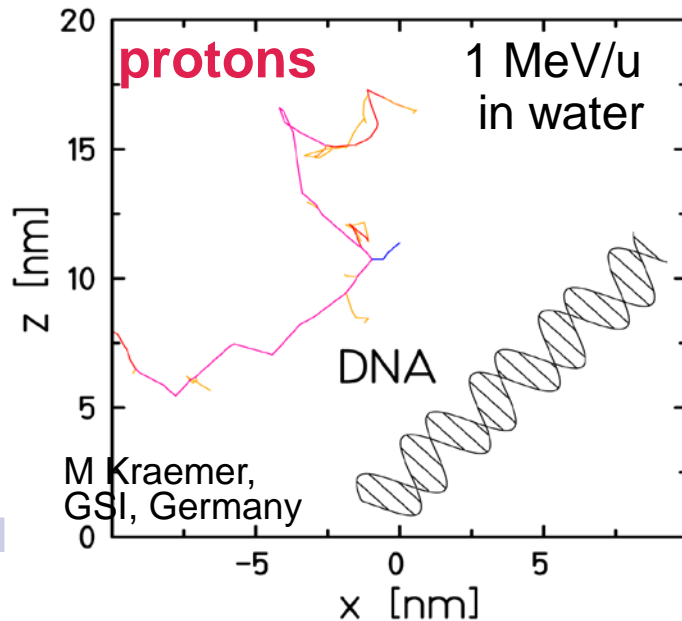


- Secondary nuclear fragments
- Secondary neutrons

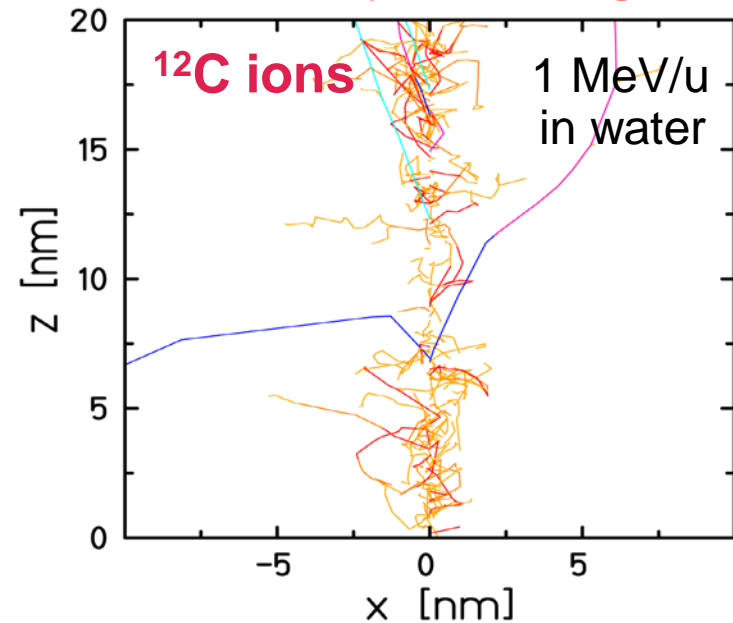


Ionization by proton and ^{12}C ion

sparsely ionising



densely ionising

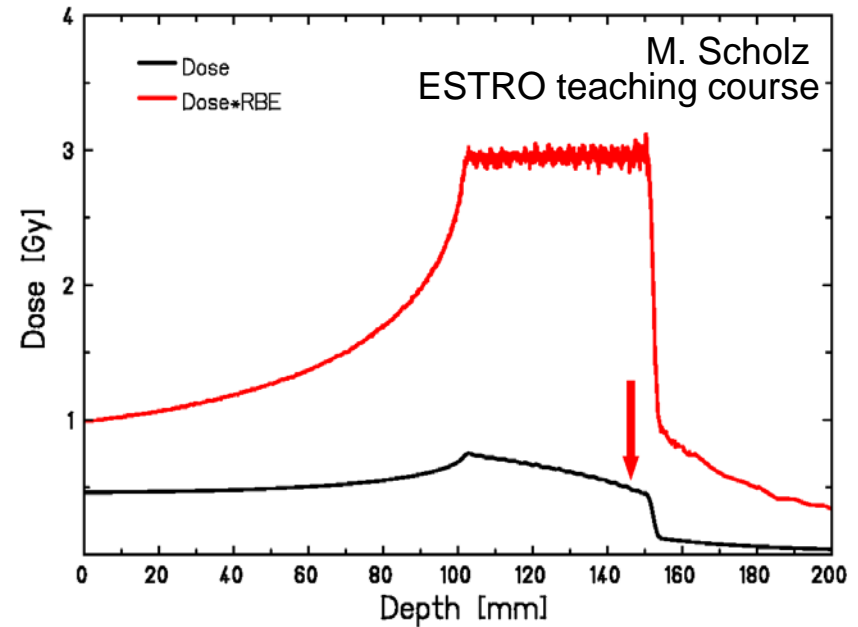
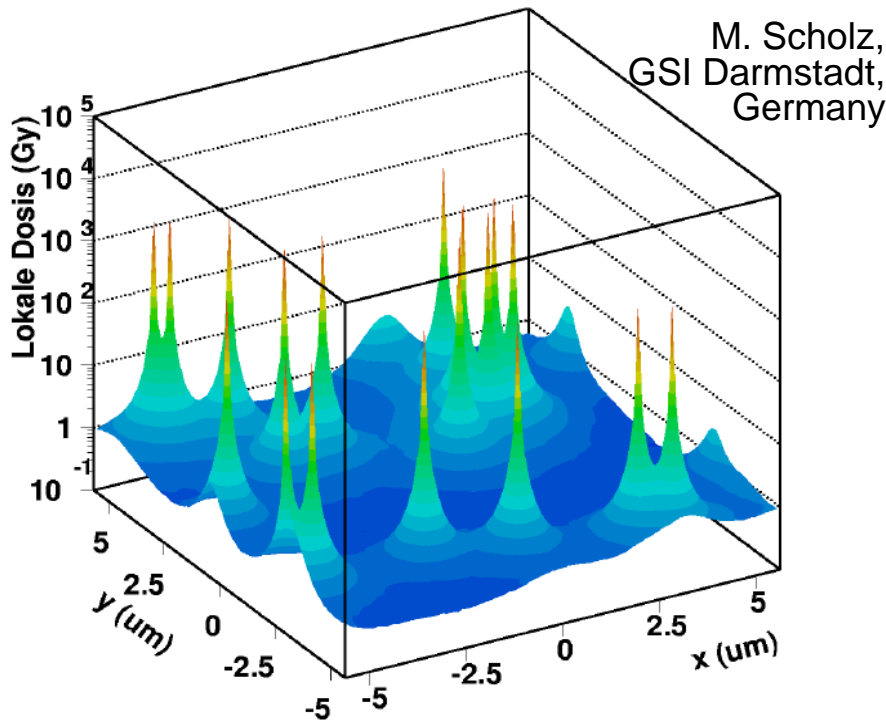


^{12}C ion in contrast to proton is producing clustered damage of DNA (i.e. many DSBs)

Local Effect Model (LEM) :cell damage by ions

Dose-deposition pattern of individual ions depends on **ion type and energy**

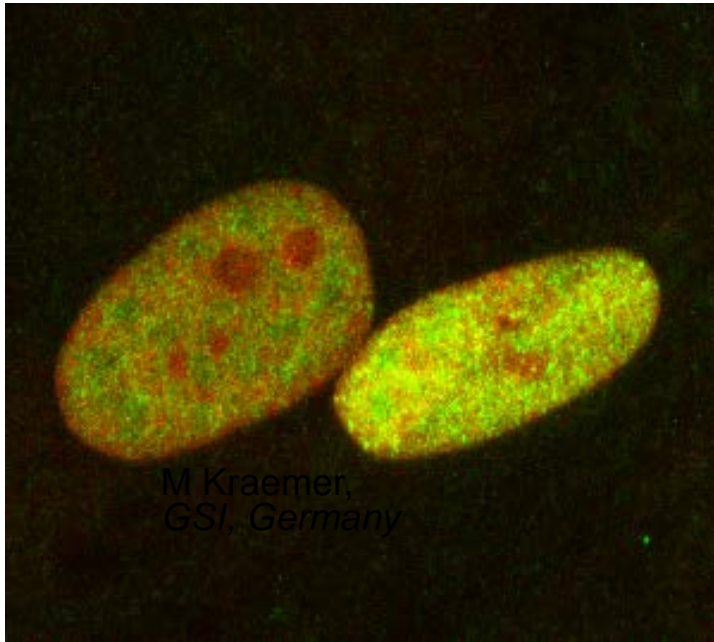
Biological effectiveness of ions depends on this pattern



Spectral composition of the beam (Z,E) and LQM for low LET radiation are input for calculations of biological dose (cell survival)

Cell damage by Gamma and Heavy Ions radiation

sparsely ionising



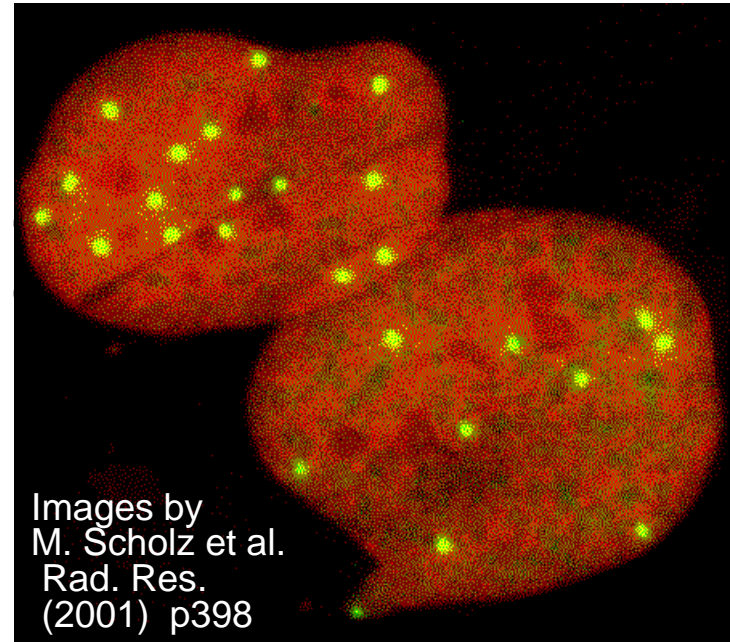
mainly **indirect DNA damage**

relative biological effectiveness:

$RBE_{\gamma}=1$

Average $RBE_{\text{protons}}=1.1$

densely ionising



mainly **direct clustered DNA damage**

irreparable DNA breaks

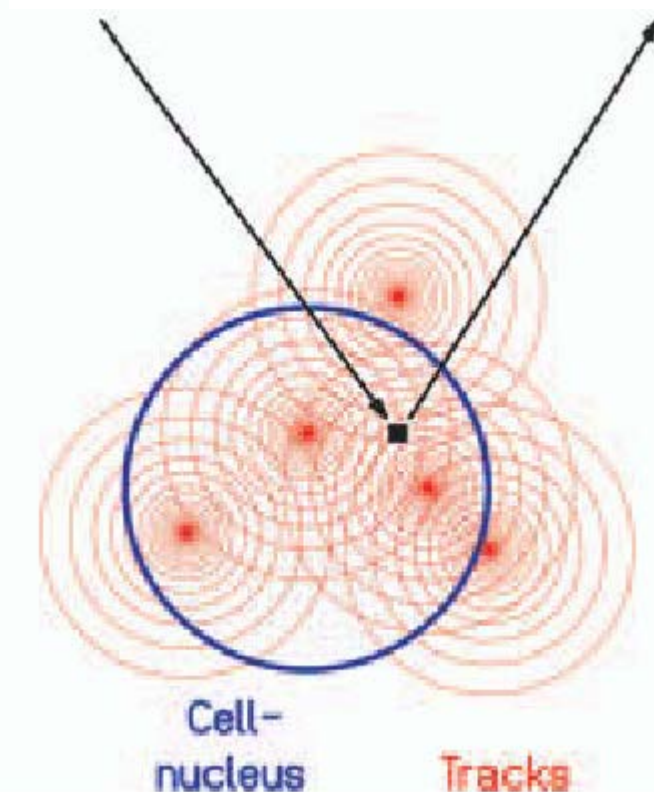
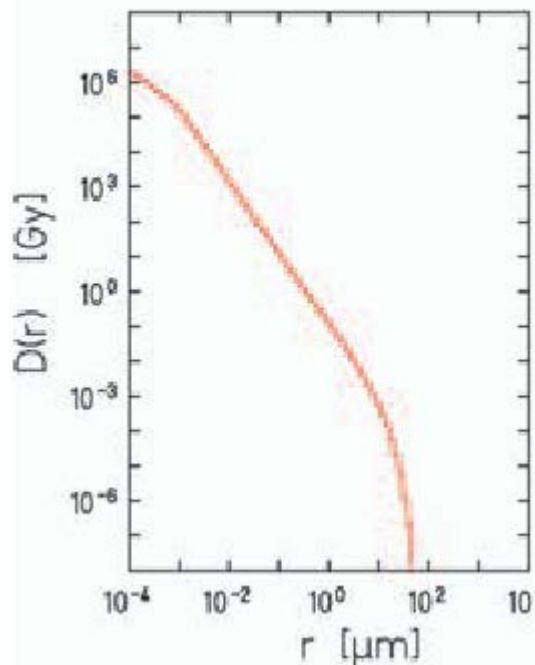
Increase of biological effectiveness

$RBE_{\text{carbon}}=2-4$

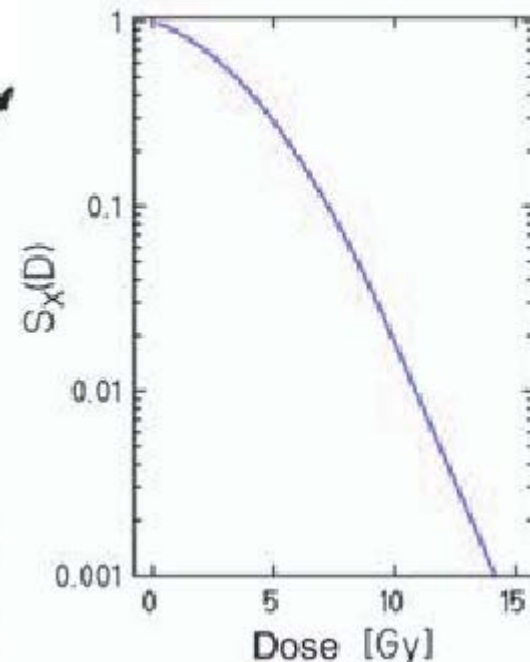
→ Radioresistant tumours!

PRINCIPLES OF LOCAL EFFECT MODEL (LEM)

Radial dose distribution



Photon dose-effect curve



- LEM is based on corresponding biological effect for X rays
- The difference in biological effectiveness between photons and charged particles is due to track structure.

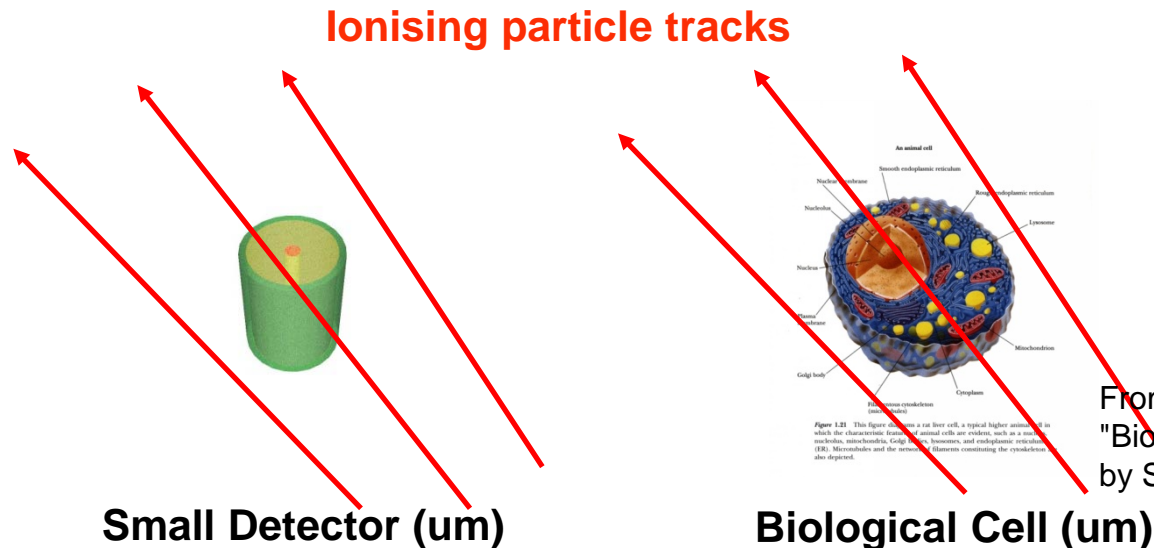
Scholz et al. , 1996

Microdosimetry and Dose Equivalent

▶ Microdosimetry

- Assumes the weighting factor is related to the energy deposited in the cell nucleus: ε
- Measure this for each particle that crosses detector
- Formulate dose distribution: $d(\varepsilon)$
- Integrate with weighting factor to give **Dose Equivalent** : $H = \int Q(\varepsilon)d(\varepsilon) d\varepsilon$
- Dose Equivalent can be used to predict biological effect of radiation

▶ We require detectors with dimensions commensurate with cell nuclei



From Garret and Grisham,
"Biochemistry" Copyright 1995
by Saunders College Publishing

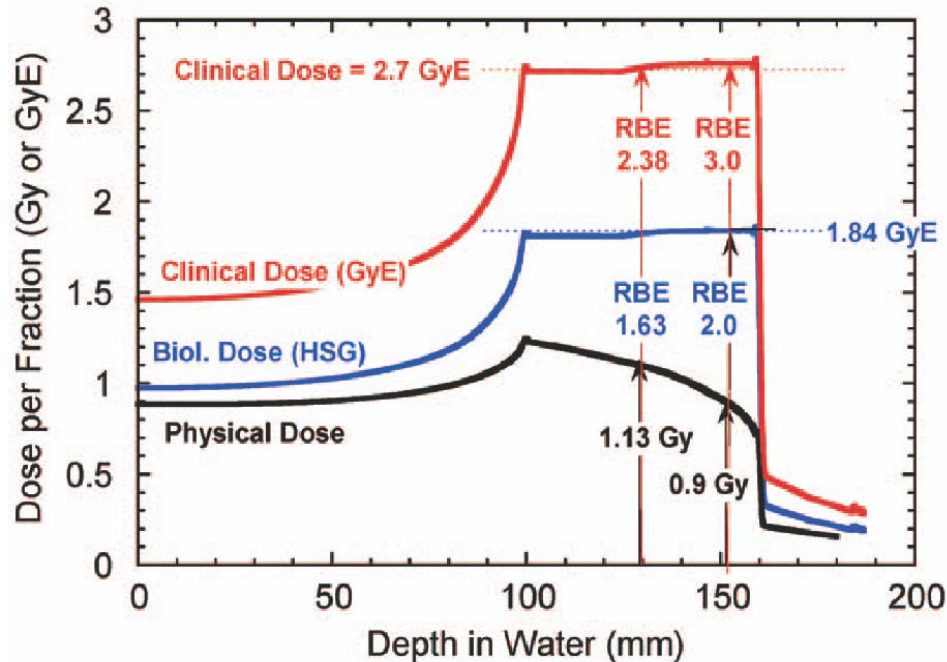
RBE₁₀

$\bar{y}_f = \int_0^{\infty} y f(y) dy$	$\bar{y}_d = \frac{1}{\bar{y}_f} \int_0^{\infty} y^2 f(y) dy = \int_0^{\infty} y d(y) dy.$
	$y^* = \frac{y_0^2 \int_0^{\infty} (1 - \exp(-y^2/y_0^2)) f(y) dy}{\int_0^{\infty} y f(y) dy}$
$S = \exp[-\alpha D - \beta D^2]$	$\alpha = \alpha_0 + \frac{\beta}{\rho \pi r_d^2} y^*$

$$RBE_{10} = \frac{2\beta D_{10,R}}{\sqrt{\alpha^2 - 4\beta \ln(0.1)} - \alpha}$$

- $\alpha_0 = 0.13 \text{ Gy}^{-1}$; $\beta = 0.05 \text{ Gy}^{-2}$; $r_d = 0.42 \text{ }\mu\text{m}$ is radius of sub cellular domain in MK model
- Where $D_{10,R} = 5 \text{ Gy}$ is 10% survival of 200 kVp X rays for HSG cells

Relative Biological Effectiveness (RBE)



HIMAC (Japan)

- Passive beam and starts using scanning beam
- RBE values are derived from in vitro experimental data in conjunction with clinical neutron experience
- RBE estimation at HIMAC is independent of the tumor type

GSI (Germany)

- Scanning beam
- RBE values for planning were estimated using Local Effect Model – LEM)
- RBE estimation are based on photon dose response curves under the cell lines

[1] O. Jäkel et al *Technology in Cancer Research & Treatment*, ISSN 1533-0346, Volume 2, Number 5, October (2003)

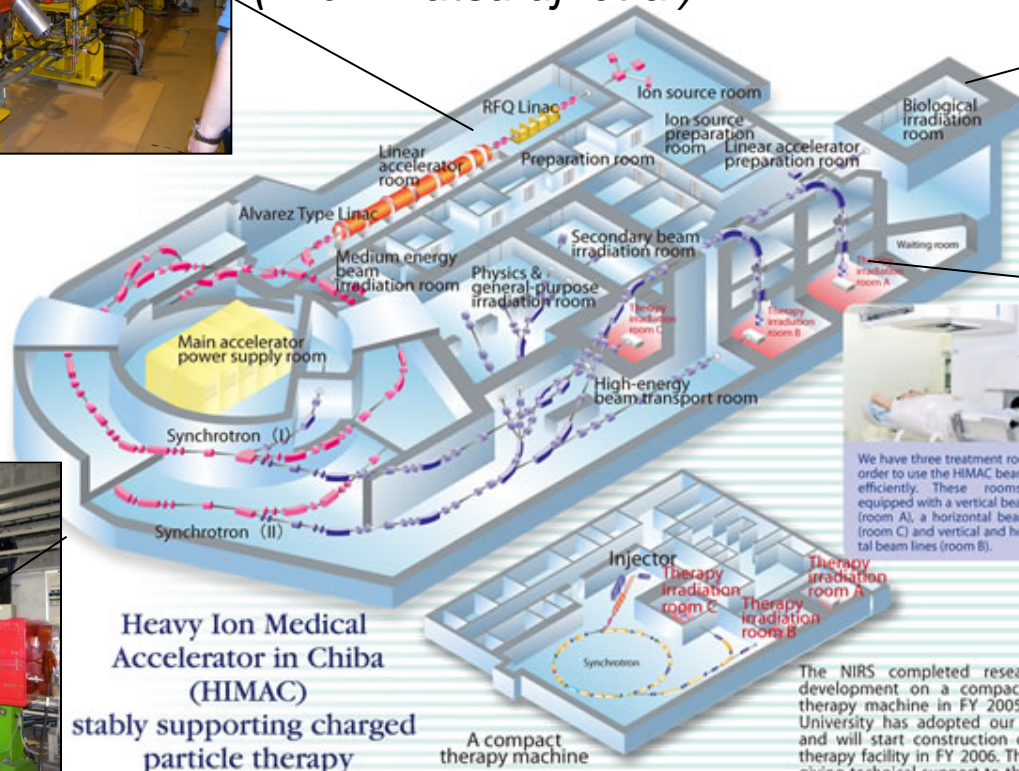
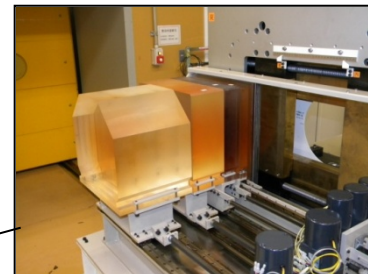
[2] O. Steinsträter et al "Mapping of RBE-weighted doses between HIMAC- and LEM-based treatment planning systems"

[3] N. Matsufuji et al *Specification of Carbon ion dose at NIRS, JRS 2007.*

HIMAC Heavy Ion Therapy facility



CMRP collaboration with NIRS, Japan
(Prof. Matsufuji et al)



We have three treatment rooms in order to use the HIMAC beam time efficiently. These rooms are equipped with a vertical beam line (room A), a horizontal beam line (room C) and vertical and horizontal beam lines (room B).

Heavy Ion Medical Accelerator in Chiba (HIMAC) stably supporting charged particle therapy

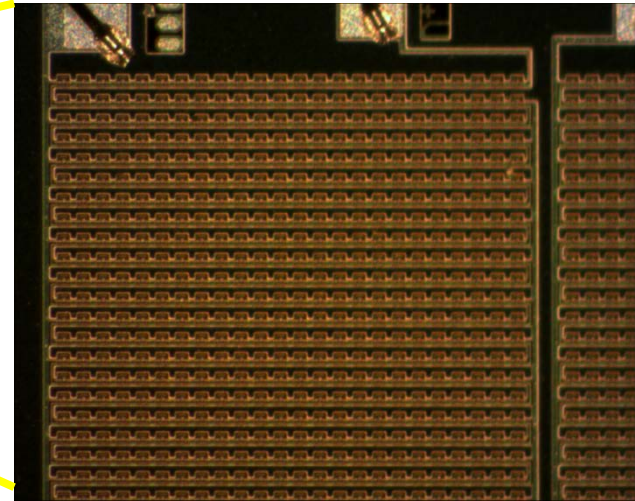
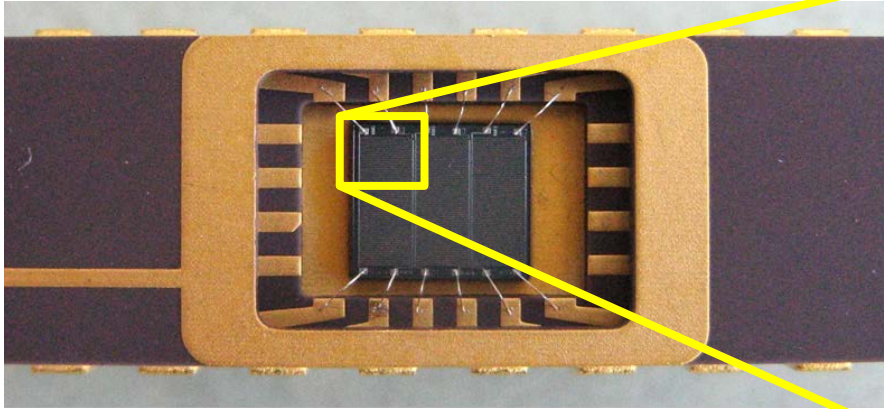
A compact therapy machine

The NIRS completed research and development on a compact carbon therapy machine in FY 2005. Gunma University has adopted our proposal and will start construction of a new therapy facility in FY 2006. The NIRS is giving technical support to this project at Gunma University.

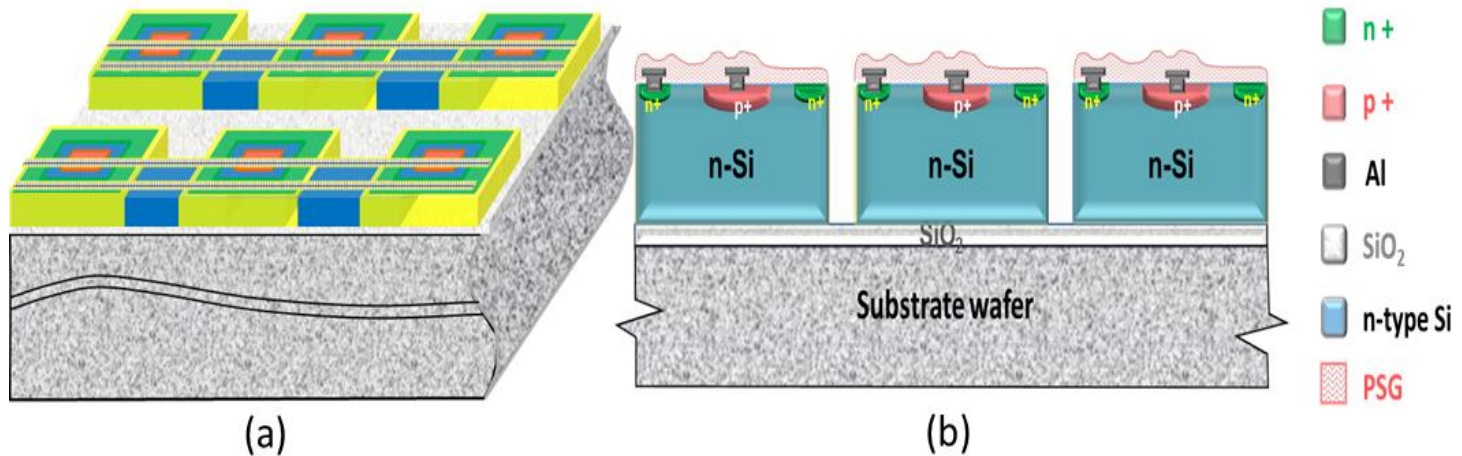


http://www.nirs.go.jp/ENG/research/charged_particle/index.shtml

3D Mesa "Bridge" Microdosimeter

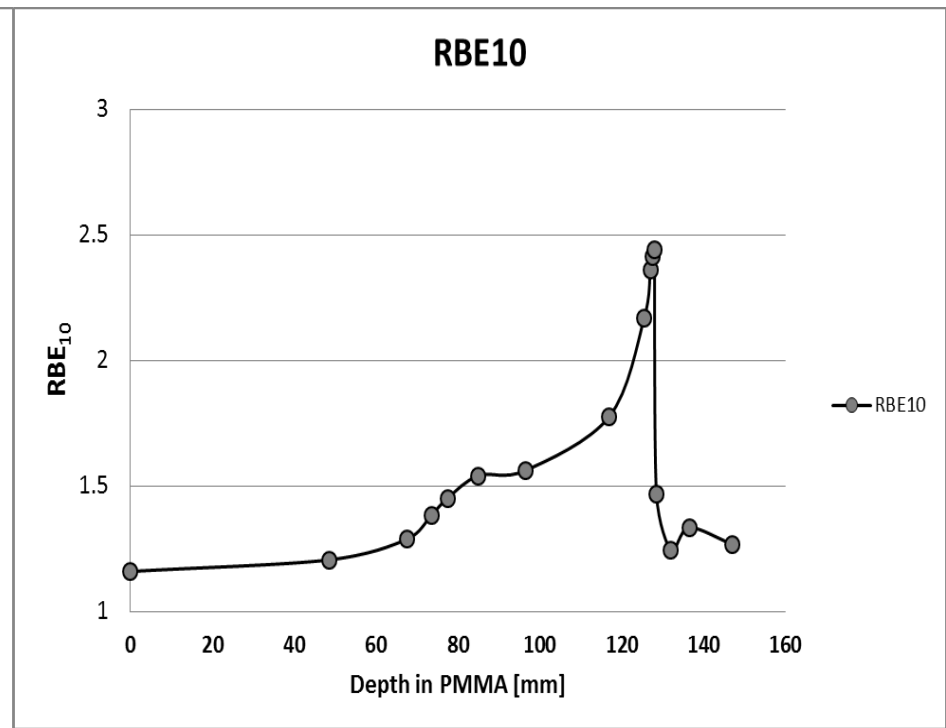
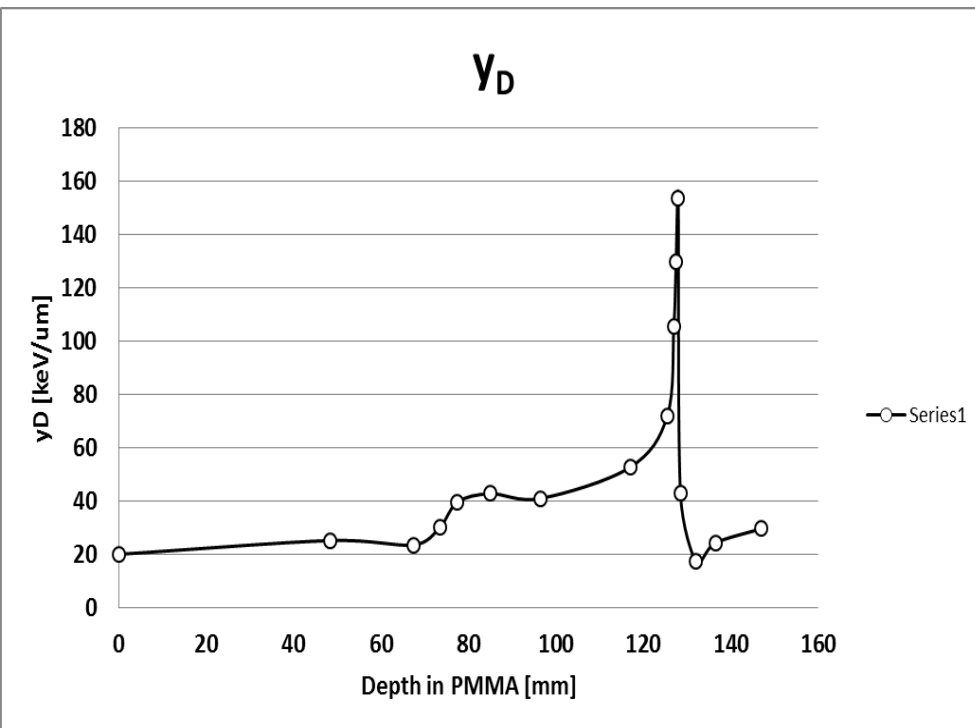


Area of whole chip : $3.6 \times 4.1\text{mm}^2$



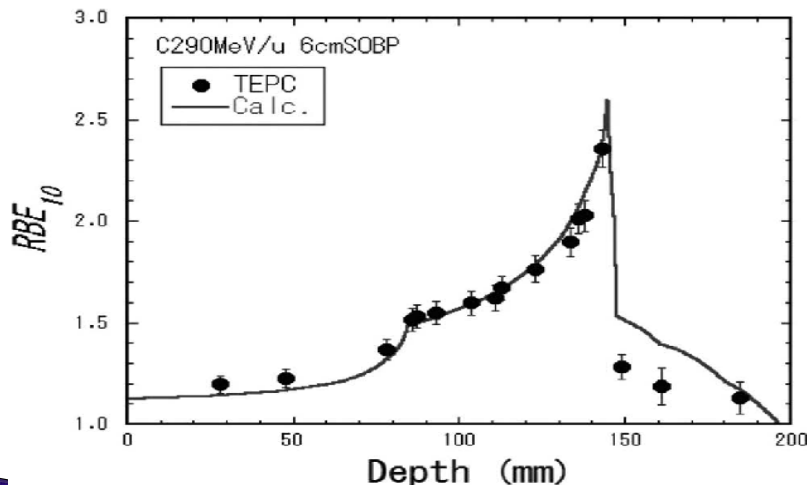
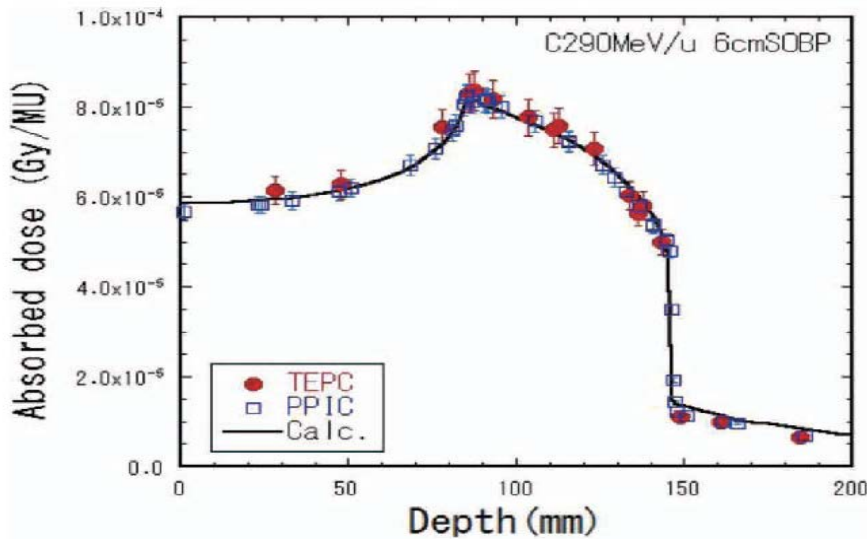
A schematic of the design of SOI bridge microdosimeter. a) 3D view, b) A cross-section of the microdosimeter behind the silicon bridge.

3D Mesa "Bridge" Microdosimeter (Results)



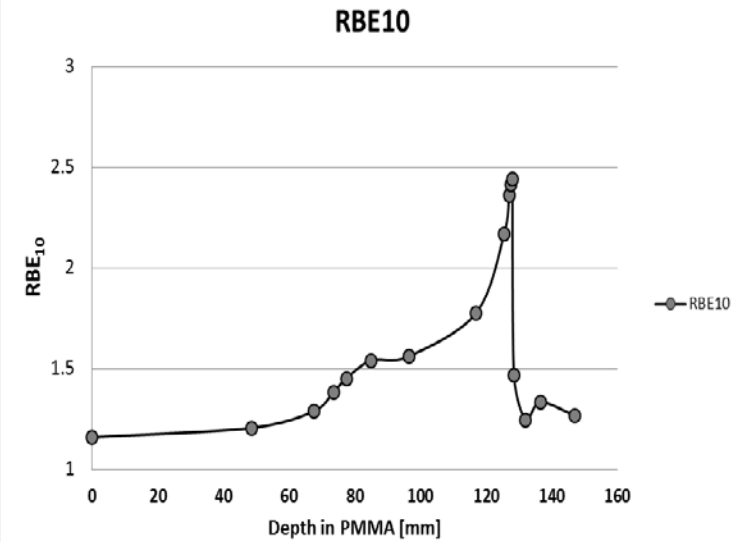
Experiment at HIMAC, Japan, May 2014

TEPC and MKM model calculation



NIRS, N.Matsufuji et al.

Measured by CMRP SOI "bridge" microdosimeter



$$\bar{y}_F = \int_0^{\infty} y f(y) dy$$

$$\bar{y}_D = \int_0^{\infty} y d(y) dy$$

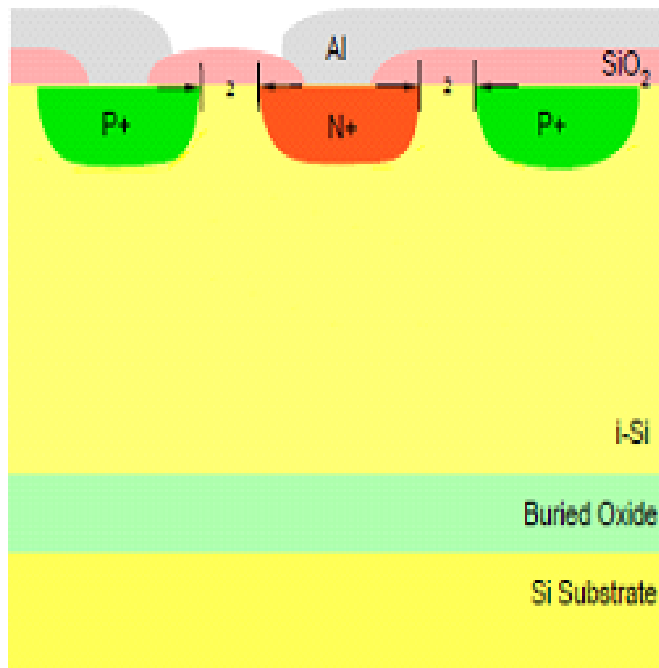
$$= \frac{1}{\bar{y}_F} \int_0^{\infty} y^2 f(y) dy$$

$$y^* = \frac{\int_0^{\infty} y_{sat} y f(y) dy}{\int_0^{\infty} y f(y) dy}$$

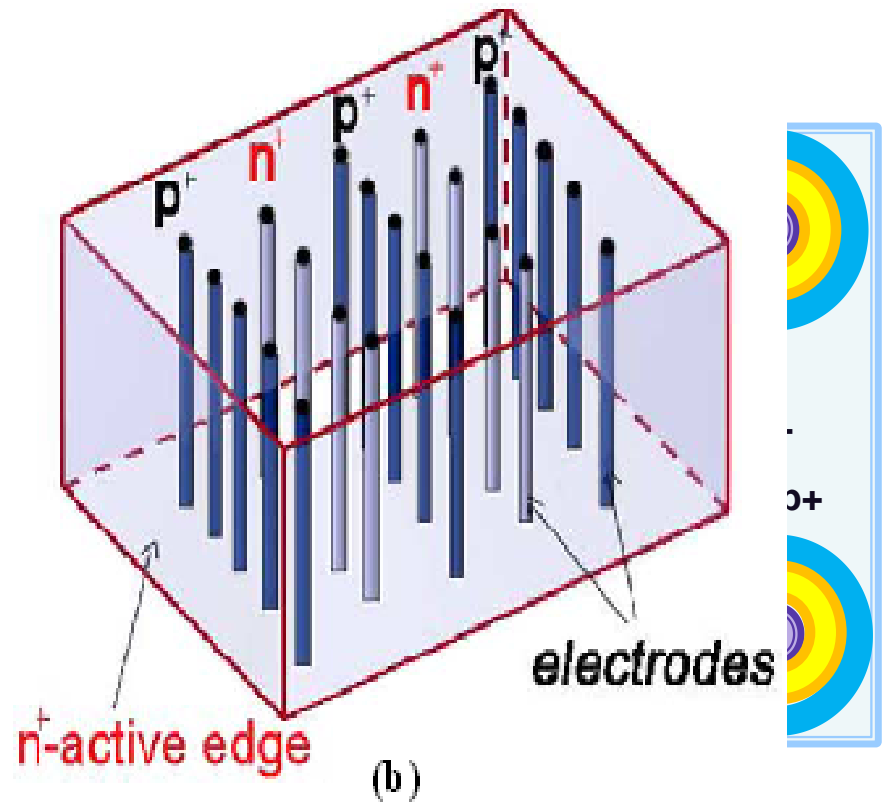
where the saturation coefficient is:

$$y_{sat} = \frac{y_0^2}{y} (1 - e^{-(y/y_0)^2})$$

NEW PROPOSED DESIGN 3D MICRODOSIMETERS DEVELOPED BY CMRP

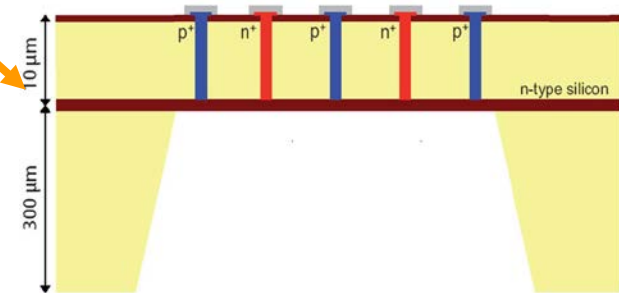
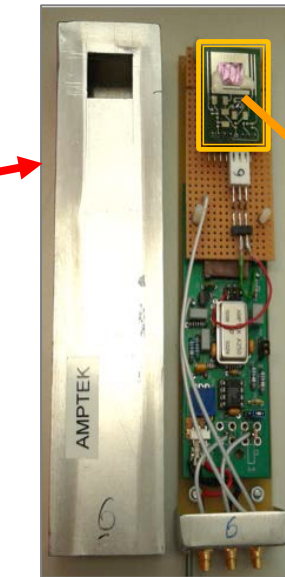
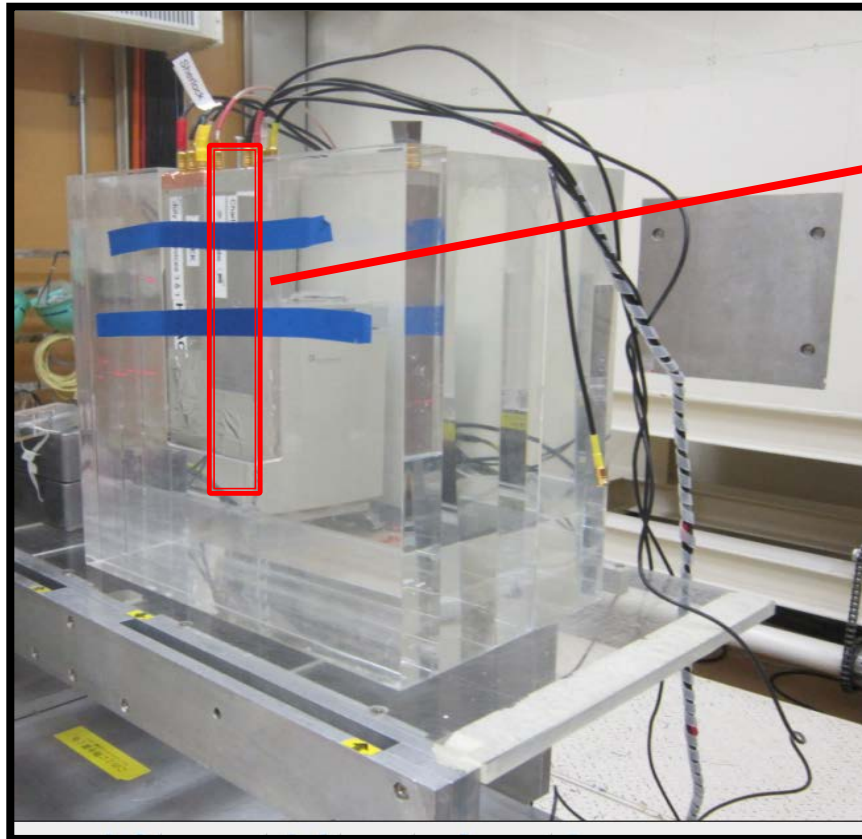


A. Cross Sectional Schematic of the Microdosimeter
(a)



- PMMA medium is filled around the sensitive volumes to produce tissue equivalent medium in order to avoid generation of secondary particles from Si lateral to SV.

Experiment for ultra-thin 3D detector with 290 MeV/u ^{12}C ion at HIMAC, 2014



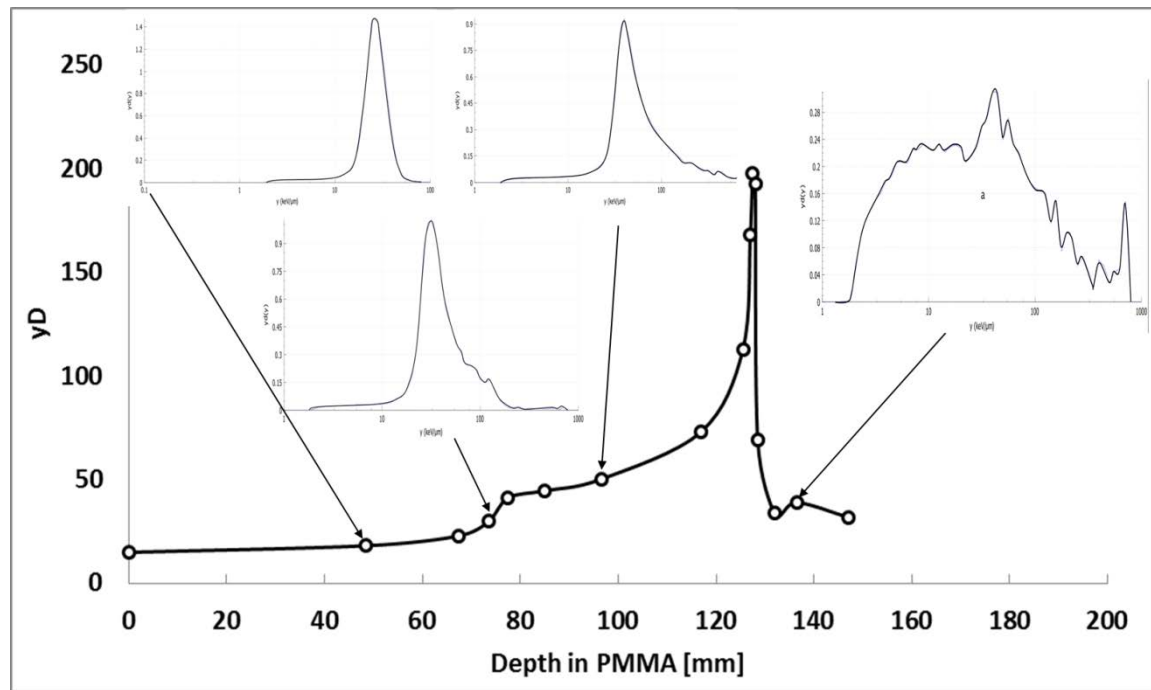
(b)

The detector is fabricated using 3D technology in 3.5 k Ω .cm n-SOI active layer followed by a thinning process which removed the 300 μm supporting wafer.

(a) Ultra-thin 3D detector connected to preamplifier and electronics

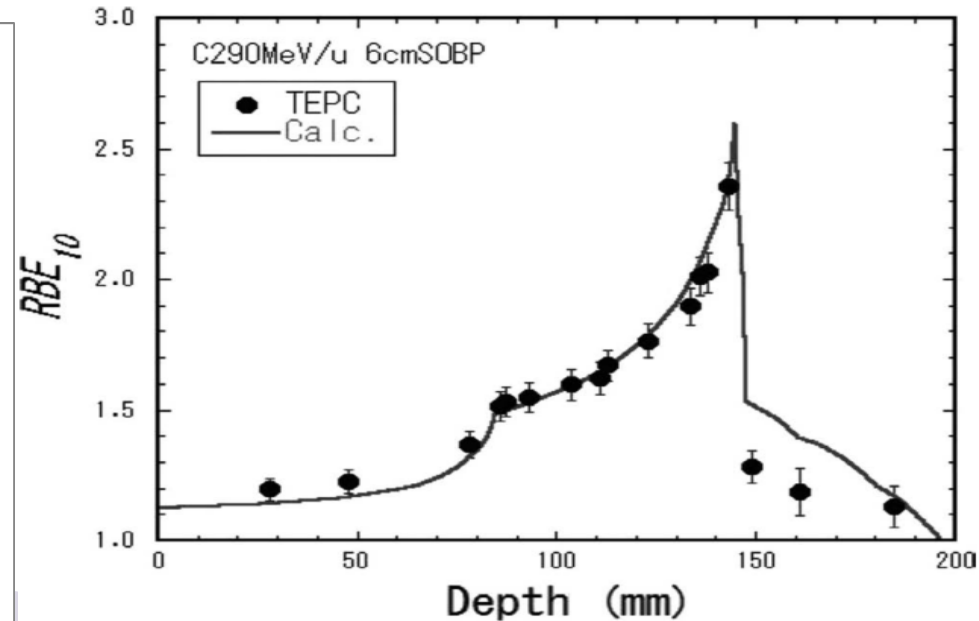
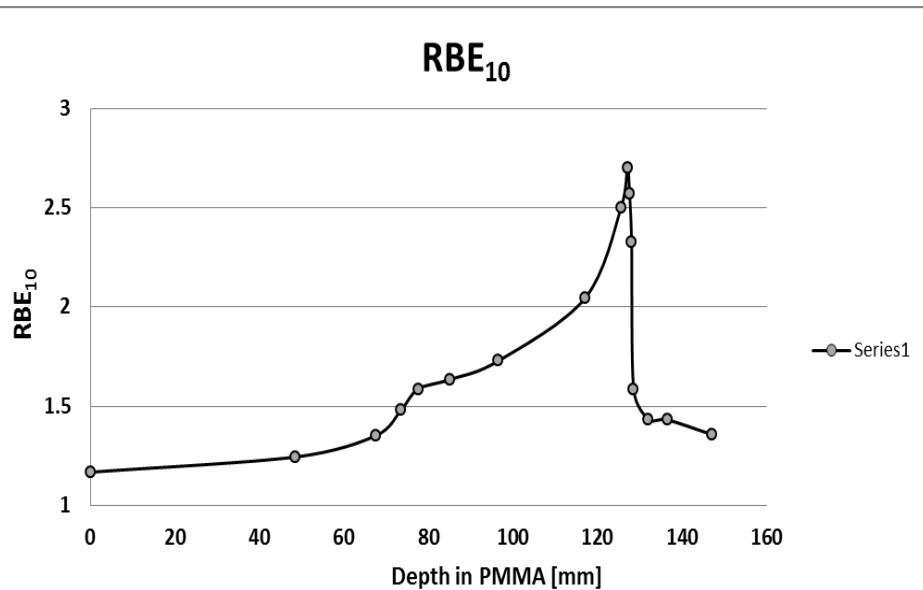
[L. Tran et al, 2014 "Ultra-thin 3D detector: Charge collection study and application for microdosimetry".]

Experiment for Ultra-thin 3D detector with 290 MeV/u ^{12}C ion at HIMAC, 2014

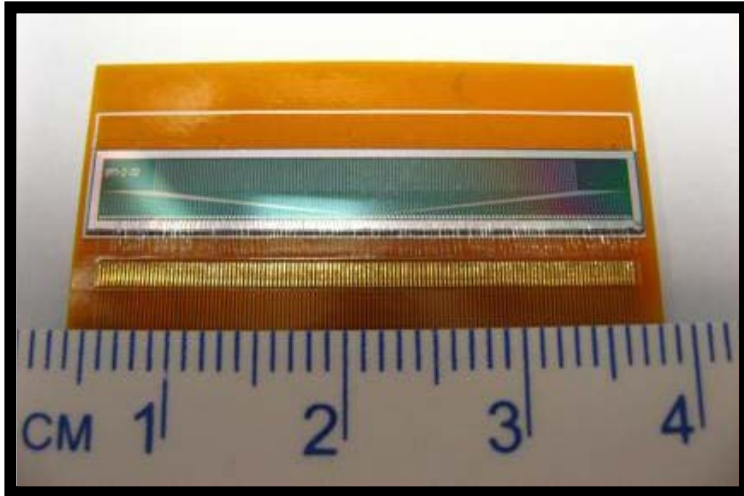


Ultra-thin 3D detector

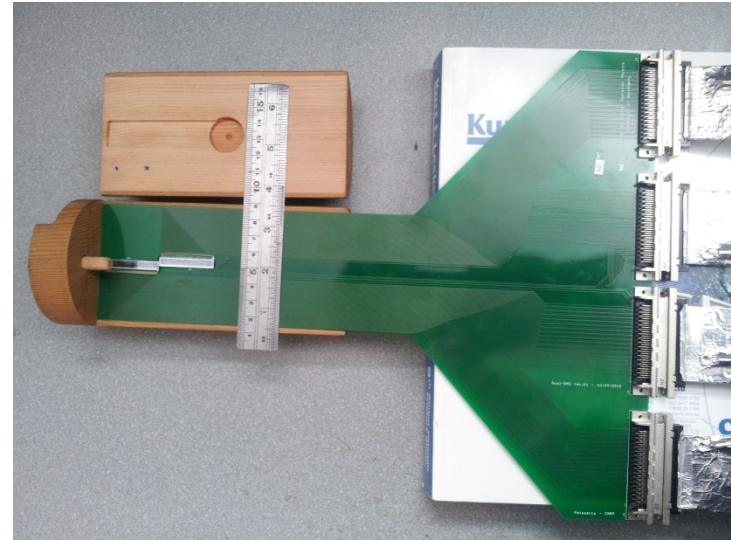
TEPC at NIRS, HIMAC



DMG: high spatial resolution dosimetry



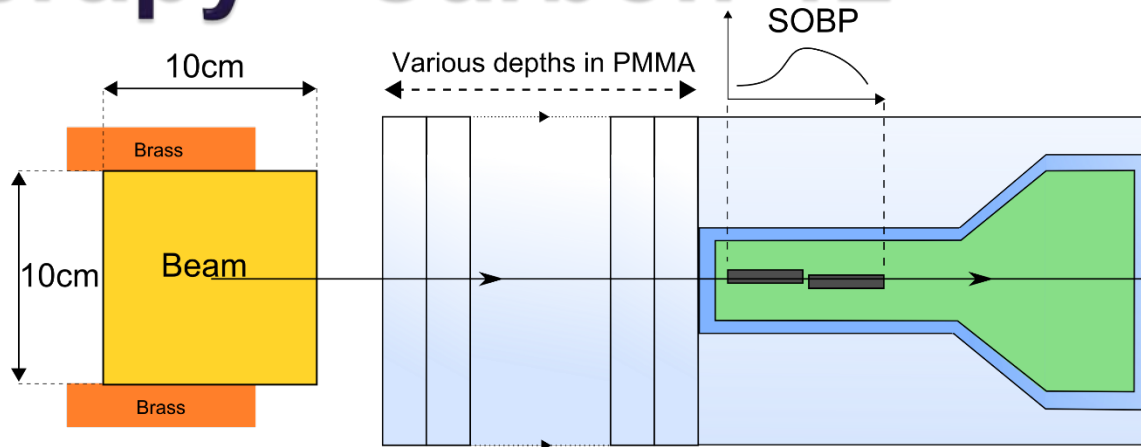
Single DMG
128 channels, pitch 0.2 mm
Total length 28 mm



Serial DMG
256 channels, pitch 0.2 mm
Total length 56mm

Heavy Ion Therapy - Carbon-12

- ▶ Experiments undertaken at National Institute of Radiological Sciences (NIRS), HIMAC facility in Chiba.

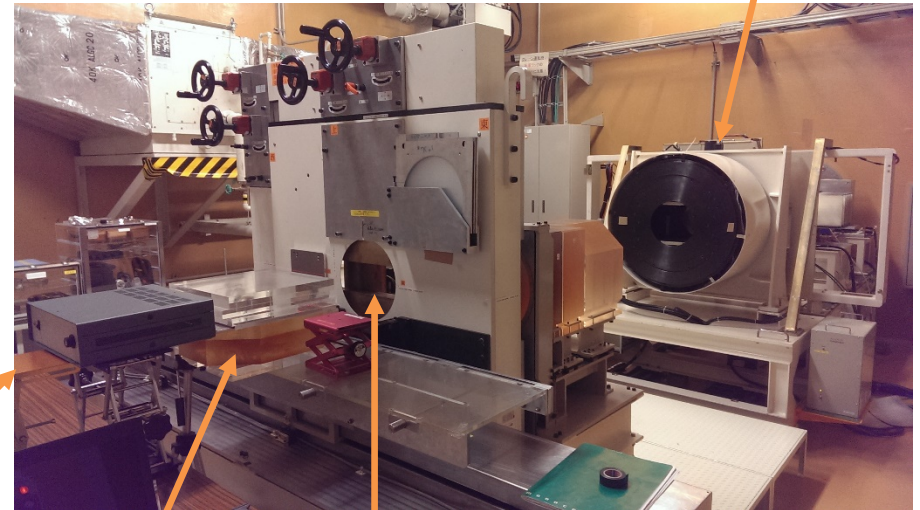


TOP VIEW

- ▶ Irradiation of Serial Dose Magnifying Glass (sDMG) with C-12 beam of energy **290 MeV/u**.

- ▶ Studies performed:

- Depth profile:
 1. Spread-Out Bragg Peak (SOBP60mm)
 2. Pristine Bragg Peak (PBP)
- Penumbral study for SOBP60mm



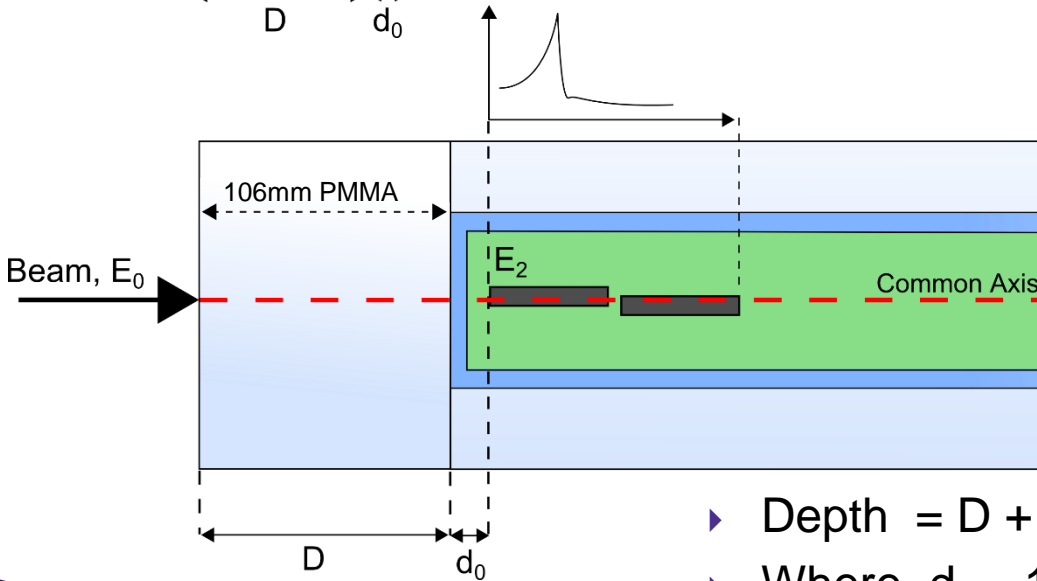
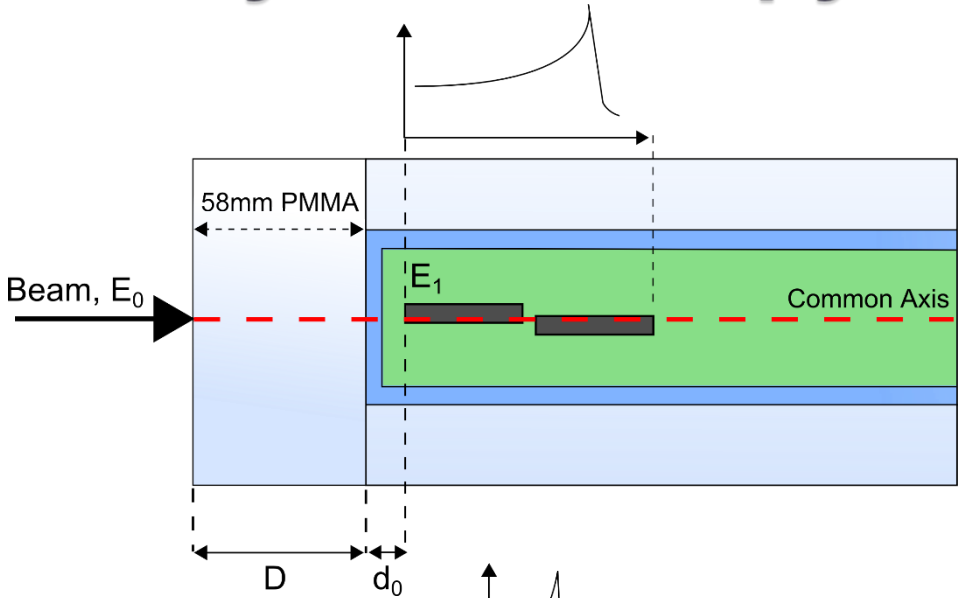
Electronics

Detector

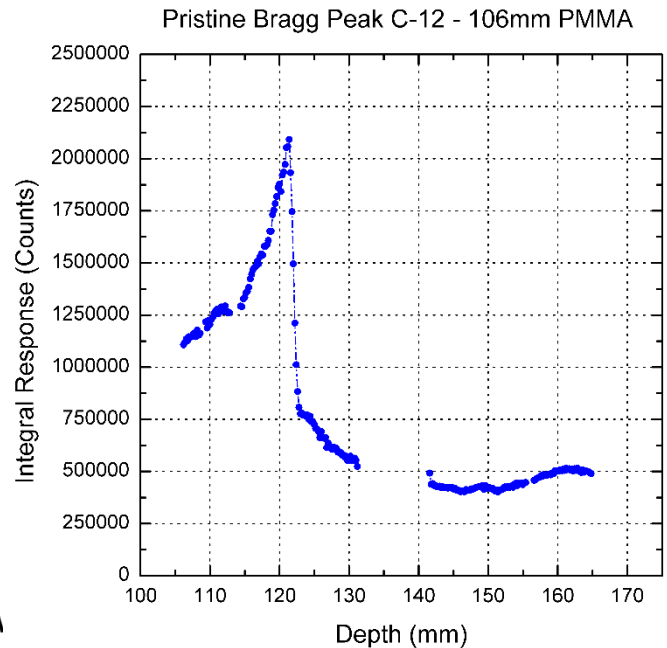
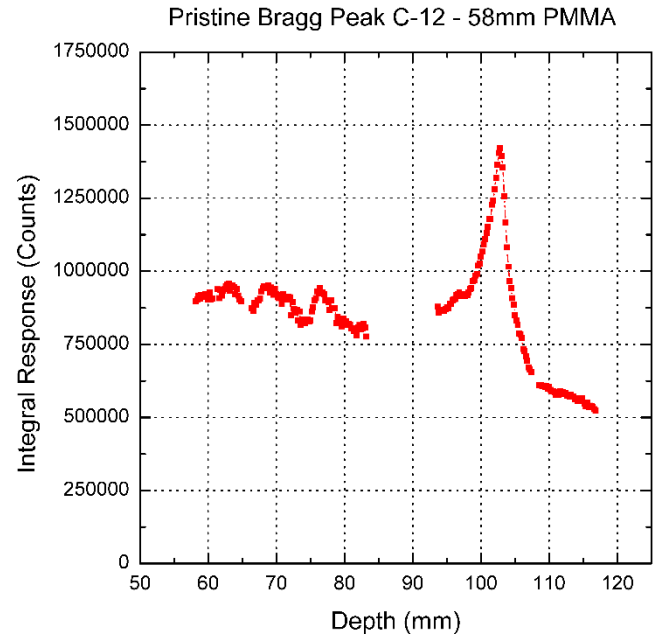
Collimator

Gantry

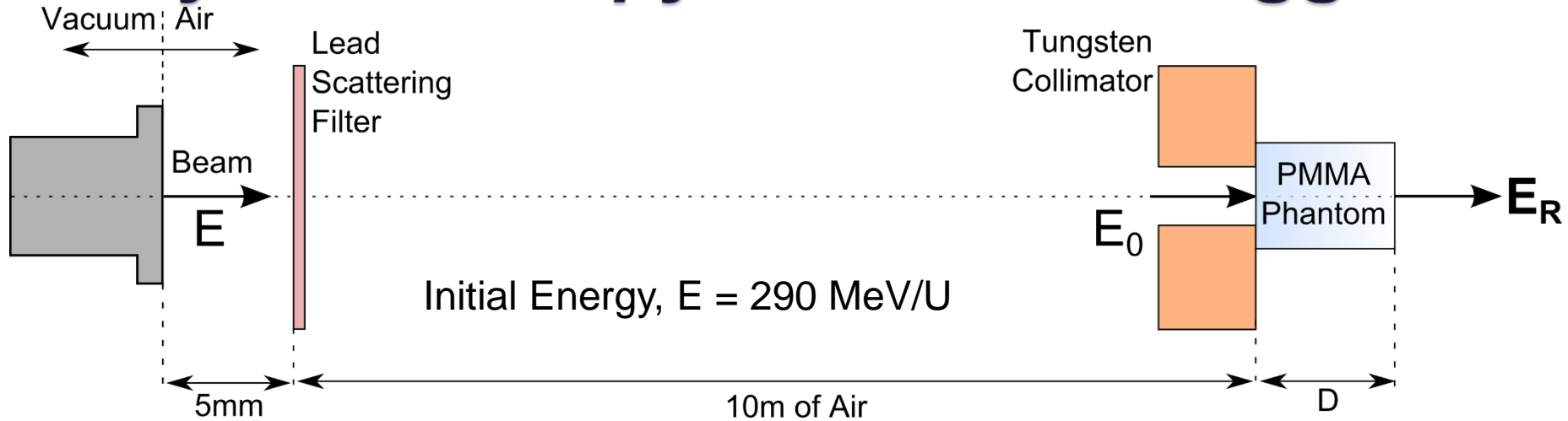
Heavy Ion Therapy – Pristine Bragg Peak



- ▶ Depth = $D + d_0$
- ▶ Where, $d_0 = 18\text{mm}$
- ▶ $D \in 40 \rightarrow 121\text{ mm}$



Heavy Ion Therapy – Pristine Bragg Peak



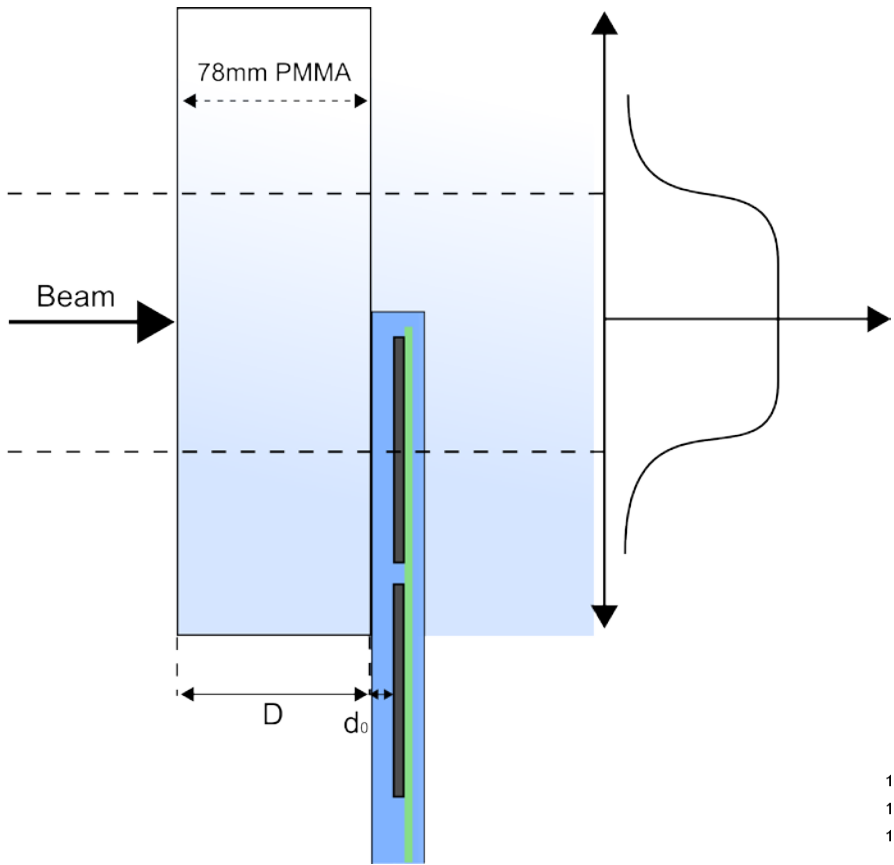
- ▶ Residual energy, E_R , for various depths in PMMA, D , reconstructed from detector measurements and compared to Monte Carlo simulation

Depth in PMMA (mm), (+/- 1 mm)	Reconstructed Residual Energy, E_R (MeV/U), (+/-3MeV/U)	Simulated Residual Energy (MeV/U), (+/-0.1%)
98	118	121
85	143	147
60	186	190
50	203	206

- ▶ Simulated $E_0=275 \text{ MeV/U}$ compared to reconstructed E_0 calculated from measured residual energies, E_R :

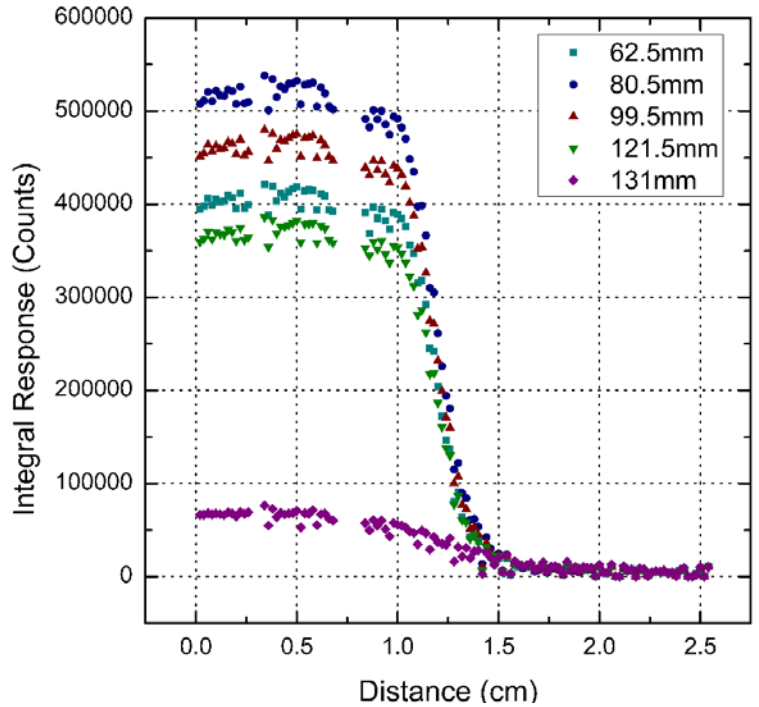
$$E_0 = (274 \pm 1) \text{ MeV/U}$$

Heavy Ion Therapy – Penumbra Study

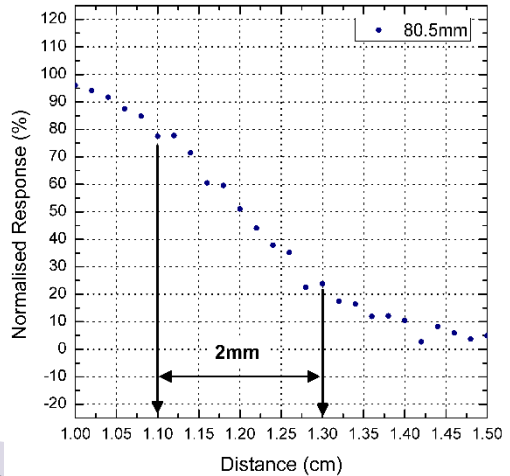


- ▶ Depth = $D + d_0$
- ▶ Where, $d_0 = 2.5\text{mm}$
- ▶ $D \in 60 \rightarrow 129\text{ mm}$

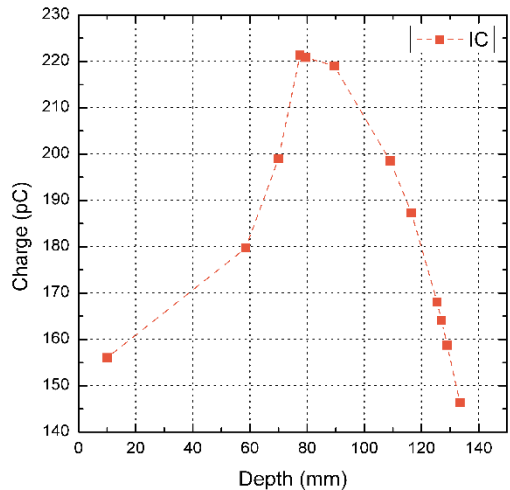
Spread Out Bragg Peak C-12 Penumbrae



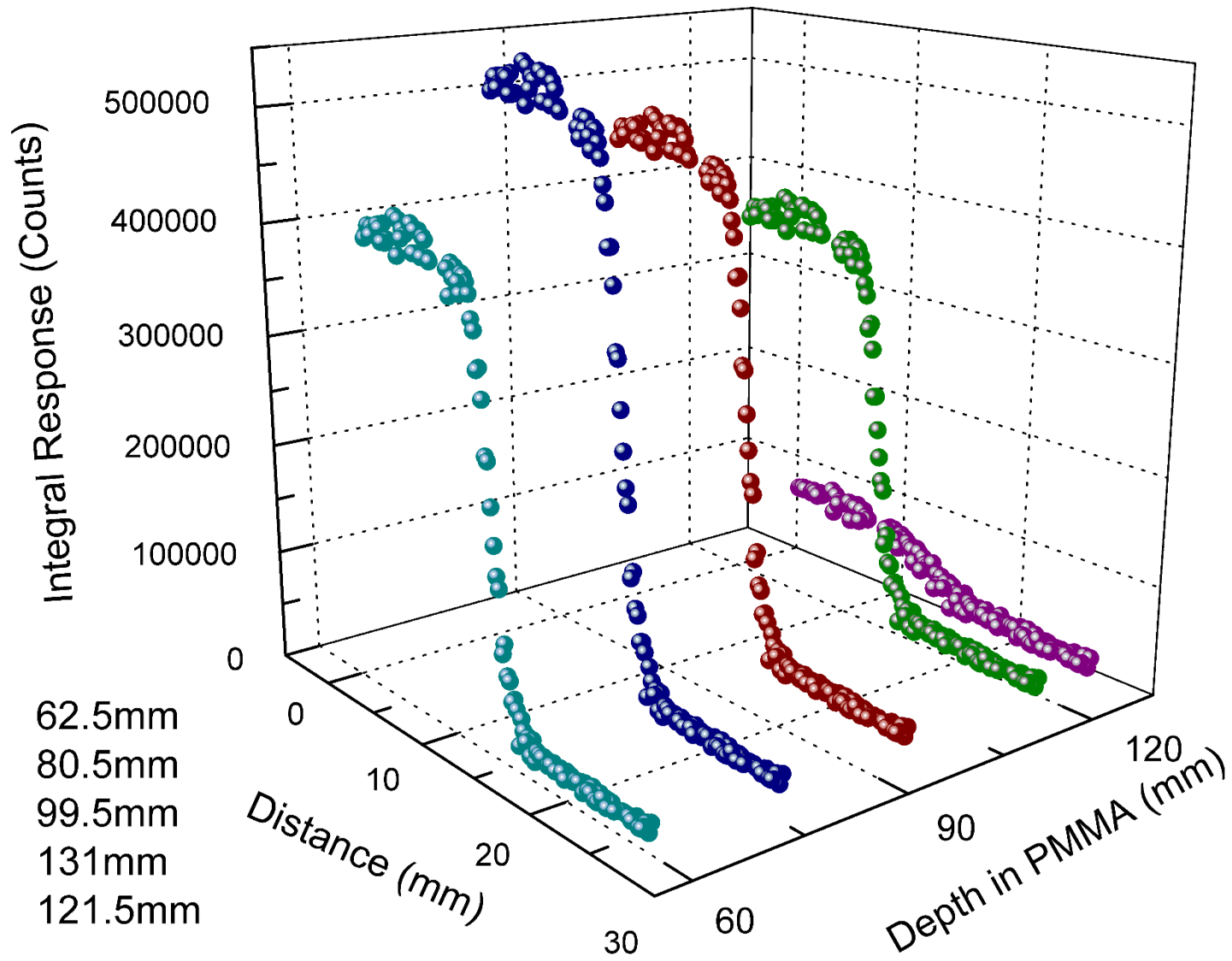
SOBP C-12 80mm Penumbrae



SOBP - Pinpoint Ionisation Chamber



Heavy Ion Therapy – Penumbral Study



Conclusion

- ▶ Semiconductor dosimeters small and real time
- ▶ High spatial resolution and skin equivalent
- ▶ Good for RT and Diagnostic Radiology
- ▶ Multiple detector redundancy
- ▶ Future of Semiconductor Dosimetry:
 - System on a Chip (detector, reader , WiHi)
 - 3D MEMS structure with well defined Q collection volume
 - Nanodosimetry –track structure measurement
 - Spectroscopy dosimetry –no need for TE material



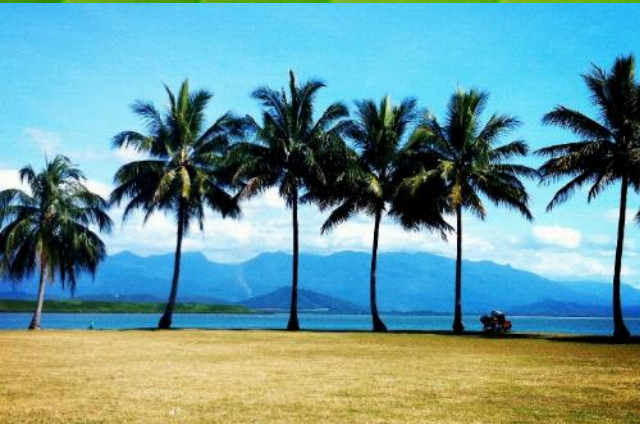
MMND & IPCT 2014

Sheraton Mirage, Port Douglas, Australia
October , 20th-25th , 2014

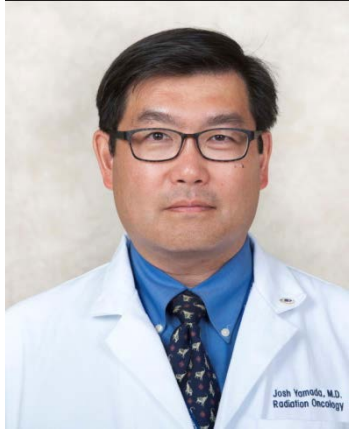
Chair: Prof Anatoly Rosenfeld
CMRP, Australia
Co-Chair: Prof Paolo Colautti
INFN-Laboratori Nazional

Dr Josh Yamada
Memorial Sloan Kettering Cancer
Centre | USA

Dr Joseph Bucci
St George CCC I Australia



MMND-IPCT 2014 Invited Speakers



Dr Josh Yamada
MSKCC

Prof Pat Kupelian
UCLA

Prof Carl Rossi
San Diego PT

Prof Hiroshi Tsuji
NIRS HIT

Prof Morten Høyer
Arthur Uni, Denmark



Prof Mack Roach
UCSF

Prof Hsiao-Ming
Lu, MGH

Dr Mauro
Carrara
National CC
Milan

Dr Michael
Scholz, GSI

Prof Reinhard
Schulte, LLU

Dr Taiga
Yamaya
NIRS PET



Thank you for
your attention!

